Kent Academic Repository
Full text document (pdf)

Citation for published version

DOI

Link to record in KAR

https://kar.kent.ac.uk/71836/

Document Version

Author's Accepted Manuscript

Pressure effect investigations on spin crossover coordination compounds

Effet de pression sur des complexes de coordination à transition de spin

By Ana B. Gaspar,[1]* Gábor Molnár,[2] Aurelian Rotaru,[3] Helena J. Shepherd[4]*

1 Institut de Ciència Molecular (ICMOL)/Departament de Química Inorgànica, Universitat de València, Edifici de Instituts de Paterna, Apartat de Correus 22085, 46071 València, Spain

2 LCC-CNRS, Université de Toulouse, CNRS, Toulouse, France.

3 Faculty of Electrical Engineering and Computer Science & Research Center MANSiD, Stefan cel Mare University, Suceava 720229, Romania

4 School of Physical Sciences, University of Kent, Canterbury, CT2 7NH, UK

Abstract: The piezo-chromic properties of spin crossover complexes have been recognized for a long time, with increasing pressure favouring the low spin state due to its smaller volume and therefore shifting the spin equilibrium towards higher temperatures and accelerating the relaxation at a given temperature. However, the interpretation and quantification of pressure induced changes have been several times compromised by the relatively poor and incomplete spectral and structural information provided by the detection methods or due to the experimental difficulties related to the need for hydrostatic conditions at low temperatures. The present review is therefore primarily focused on these experimental aspects of high pressure spin crossover research providing an overview of methods of pressure generation and associated detection methods as well as on selected recent results.

Résumé : Les propriétés piézo-chromiques de complexes à transition de spin ont été identifiées depuis longtemps. Du point de vue théorique, l'application d'une pression favorise l'état bas spin, de plus petit volume. Ainsi les températures de transition augmentent et les cinétiques de relaxation s'accélèrent sous pression. Toutefois, l'interprétation et la quantification des modifications induites par la pression restent un challenge en raison de la difficulté d'obtenir des données structurales et spectrales fiables dans des conditions de pression hydrostatique. Ceci est d'autant plus vrai lorsque les hautes pressions et les basses températures doivent être combinées. Ainsi, l'objectif principal du présent article est une mise au point sur les techniques utilisées pour l'étude des composés à transition de spin sous pression – illustrées par une sélection de résultats récents.

1. Introduction

Molecular spin crossover (SCO) complexes are known to be very sensitive to external pressure because of the large difference in volume ($\Delta V_{HL} = V_{HS} - V_{LS}$) between the high spin (HS) and low spin (LS) isomers. While the volume of the coordination octahedron is always modified by virtually the same ratio – ca. 25 % for complexes with $Fe^{II}N_6$ coordination core – the unit cell volume modification that reflects the macroscopic change strongly varies from one complex to the other [1]. This is in part a result of anisotropic structural response of these materials that are often of low symmetry, although the difference in volume is always noteworthy (several %). Hence, for relatively small applied pressures (i.e., a few hundred bars) the work term, $p\Delta V$, of the Gibbs' free energy is already significant. For this reason, pressure tuning the spin-state of SCO compounds has been a valuable experimental tool since the early stages of SCO research and continues to attract significant attention from researchers.

High-pressure spectroscopic studies of Drickamer and Ferraro [2–20] in the 60's-70's had already addressed the SCO phenomenon using Mössbauer, UV-VIS and IR spectroscopies associated with either piston-cylinder or anvil-type pressure cells. High-pressure investigations (primarily using Mössbauer spectroscopic detection) were then taken up in the 80's by the groups of Gütlich, Long and König [21–41]. There was a renaissance of interest in the effect of pressure on SCO compounds during the 90's [42–77], involving studies using either clamp-type and helium gas cells coupled to magnetic susceptibility [26] and optical [49,60] detection methods or diamond anvil cells (DAC) in conjunction with X-ray spectroscopic[61,64,66,70] or X-ray diffraction [68,78] techniques. These and also some more recent studies that we will discuss have led to a range of experimental observations on several dozens of SCO compounds. Besides the exploration of the p-T phase diagram, numerous investigations were also conducted to elucidate pressure effects on spin-state relaxation phenomena as well [28,33,36,38,41,52,57,58,63].

In a first approximation one can describe the pressure effects on spin crossover systems by expressing the HS − LS energy gap as $\Delta E_{HL}(p) = \Delta E_{HL}(p=0) + p\Delta V_{HL}$. The pressure dependence of the spin transition temperature (Tc) is given then by the Clausius-Clapeyron equation:

$$\frac{\partial T_c}{\partial p} \;=\; \frac{\Delta V_{HL}(p)}{\Delta S_{HL}(p)} \qquad (1)$$

where $\Delta S_{HL}(p) > 0$ is the entropy change (of mainly vibrational origin) accompanying the spin crossover. Using this approximation, a linear shift of the transition to higher temperatures (typically by as much as 100-200 K/GPa) and also a decrease of the hysteresis width (or the abruptness of the transition curve) can be predicted with increasing pressure. While these trends have often been confirmed, the experimental observations do not always fit these expectations. The reason for this is that pressure is coupled to the spin-state of the system not only by the work term, but by several other mechanisms as well. In particular, structural changes may also occur under the effect of an externally applied pressure leading to a non-linear and non-isotropic decrease of the volume with the decreasing HS fraction, and eventually to the change of the space group or modulation of the lattice. Moreover, the pressure effects on the lattice dynamics (elastic moduli, phonon frequencies) may be also significant, but remain generally unknown. These parameters are obviously important in determining $\Delta V_{HL}(p)$ and $\Delta S_{HL}(p)$, but even more importantly they may have a crucial effect on the interactions between the molecules, i.e. on the cooperativity of the SCO. In general,

unexpected pressure effects on the spin transition temperature or the hysteresis width are thus attributed *ad-hoc* to pressure induced changes of the crystal structure and/or lattice dynamics. For this reason the need for combined structural, macroscopic (e.g. magnetic or optical) and spectroscopic analysis has been clear for a long time, but such studies unfortunately remain scarce in the SCO field [79,80].

On the whole, pressure effects also remain less investigated compared to thermal and light induced spin-state changes, due mainly to experimental difficulties of working under hydrostatic pressure and variable temperature at the same time. In addition, the experimental high pressure setups are, in most cases, home-made and the associated know-how for their use remains to some extent confidential for their rather specialized features. Much of the technical literature concerning high pressure experimental methods relates to research at pressures well in excess of the relatively modest pressure range typically encountered in SCO research. For these reasons, the primary aim of the present review is to assess the experimental aspects of high pressure SCO research, which will be then illustrated by selected examples.

While we restrict the scope of this contribution to the effects of in-situ, externally applied pressure, it is important that readers be aware of the conceptually related area of research into the effect of so-called *internal pressure* in SCO systems. Doping a SCO material with metal ions of a different ionic radius exerts an internal pressure on the lattice (either positive or negative depending on the size of the guest ions with respect to the host), and produces a concomitant shift in $T_{1/2}$, that can be enhanced or negated through the application of external pressure [55,81].

2. Experimental Methods

Molecular-based spin crossover compounds are relatively soft, and as such they are particularly sensitive to shear stress caused by the presence of non-hydrostatic environments [82]. SCO materials are notoriously sensitive to the presence of lattice defects, and so the possibility of inducing these by non-hydrostatic pressure must be assessed in any high pressure experiment. As such, it is important to consider carefully the experimental methods used to generate high pressure during investigations of these systems.

2.1 High Pressure Generation

Techniques for the generation of high pressures for individual experiments are dictated both by the pressure range of interest for the material and the experimental technique employed [83]. The pressure range of interest for molecular-based SCO materials ranges from atmospheric to c.a. 5 GPa, and thus the discussion presented here is limited to this relatively 'low' high pressure regime. It should however be noted that pressures up to the megabar (1 GPa = 10 kbar = 0.01 Mbar) range can be achieved experimentally, and while these extreme pressure ranges are far in excess of those of interest for the majority of molecular spin crossover studies, they are successfully exploited by geophysicists in the study of spin transition processes occurring in minerals within the temperature and pressure ranges relevant to the Earth's interior [84,85]. In this section we will introduce the most commonly employed methods for generating high pressure that have been used in the study of SCO materials. It is not intended to be an exhaustive review, but rather designed to serve as a tutorial for newcomers to the experimental study of SCO materials at high pressure.

As a general concern for all kinds of pressure cells, the choice of hydrostatic pressure transmitting medium may be dictated by the pressure and temperature range of interest, the transparency to the characterisation technique, ease of loading and chemical solubility/reactivity with regards to the sample. It should also be noted that the sensitivity of many SCO materials to the presence of certain guest molecules may well be another important factor in the choice of pressure transmitting medium. Typical media include silicone oils, a mixture of methanol/ethanol, helium gas, liquid helium or other condensed gases [86,87]. In some cases, the relatively soft polycrystalline SCO complexes were even successfully compressed without any additional pressure transmitting medium [88].

Another common problem is the determination of pressure inside the cells. (*N.B.* The particular case of pressure determination with piston-cylinder cells and capillary fed 'low-pressure' cells is discussed separately in the next sections). Whenever optical access is available to the sample chamber the pressure inside the cell is most commonly determined by measuring the position of the R_1 fluorescence line of a small ruby chip or sphere located inside the sample chamber [89], as shown in Figure 1, which shifts with applied pressure according to equation 2 [90],

$$P = 1870\epsilon[1 + 5.9\epsilon], \ \epsilon = \frac{\lambda}{\lambda_0} - 1 \qquad (2)$$

where λ and λ_0 represent the wavelength of the R_1 fluorescence line at elevated and ambient pressure respectively, and the pressure, P, is given in GPa. It is also possible to determine the pressure inside the cell using the diffraction pattern of a known internal standard such as gold, NaCl or quartz, which may be more convenient than ruby for determining the pressure during diffraction experiments, where the diffraction pattern of the standard can be measured simultaneously with that of the sample [91].
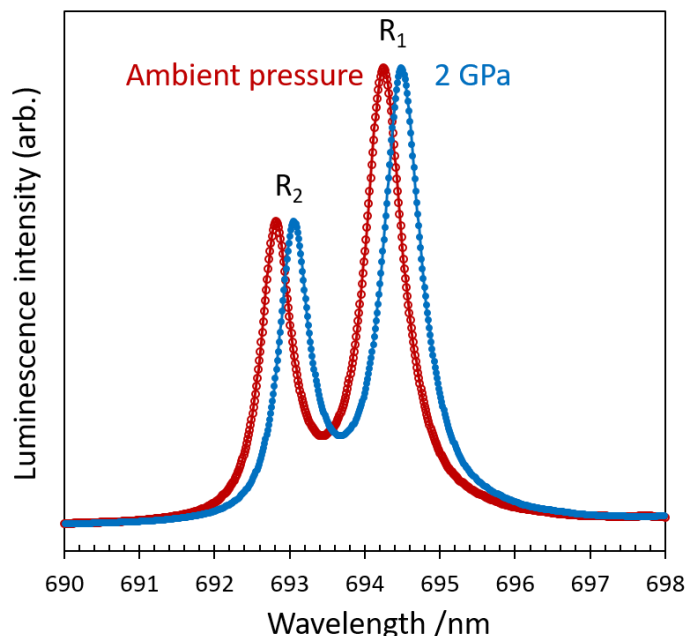

Figure 1. Illustration of the shift in position of the R1 fluorescence line of ruby on increasing pressure from ambient pressure to 2 GPa at room temperature

Reproducible phase transitions of some materials can be also used as a pressure gauge. Of particular relevance to the SCO field is the pressure dependence of the superconducting transition of Sn or Pb, which is commonly used to infer the applied pressure in magnetometry experiments, as illustrated in Figure 2. In this case, a small piece of high purity

metal is placed inside the cell and the precise transition temperature is recorded. The pressure (up to 5 GPa) is determined according to the following analytical expressions, as presented in [92]:

Pb
$$T_c(P) = T_c(0) - (0.365 \pm 0.003)P \qquad (3)$$

Sn
$$T_c(P) = T_c(0) - (0.4823 \pm 0.002)P + (0.0207 \pm 0.0005)P^2 \qquad (4)$$

In
$$T_c(P) = T_c(0) - (0.3812 \pm 0.002)P + (0.0122 \pm 0.0004)P^2 \qquad (5)$$
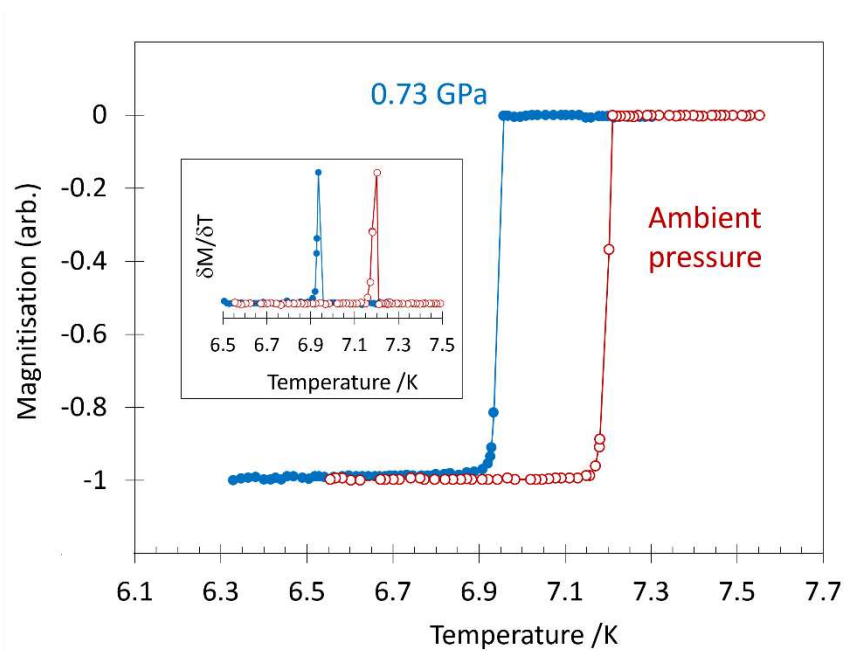
Figure 2. Illustration of the shift in temperature of the superconducting transition of Pb on the application of pressure from ambient to 0.73 GPa

The typical accuracy of these various pressure gauges is rarely better than approx. 0.05 GPa and depends strongly on the instrumental resolution as well as on various other experimental conditions – most crucially on the investigated pressure and temperature range. This level of accuracy remains an important concern for the SCO research where the applied pressure frequently remains below 1 GPa. In this context the use of electrical gauges may be particularly advantageous. In particular, four-wire resistance measurements using tiny manganin wires can provide very precise pressure readings (better than 0.01 GPa). In addition the pressure dependence of the manganin resistance is only very weakly temperature dependent.

Temperature variations not only complicate pressure calibrations, but problems of hydrostaticity may substantially increase at low temperatures. It is thus useful to note that with some care most pressure gauges allow for detecting the loss of hydrostaticity. To this aim one can either measure the pressure gradient across the cell using several gauges (e.g. ruby chips) or analyse peculiar changes in the behaviour of the gauge. For example, the decreasing sharpness of the Pb superconducting transition or the broadening of the ruby lines are symptomatic of shear stresses.

Before going into further details a word of CAUTION is necessary here. Potential danger from high pressure apparatus must be always carefully evaluated - even when using certified commercial equipment – and appropriate safety

measures must be taken. Perhaps surprising at first sight, but the most dangerous equipment is often moderate - low pressure vessels. Indeed, the danger is not linked to the magnitude of the applied pressure, but to the potential energy stored during compression. Key factors are the volume and the compressibility of the pressurized medium. For example, diamond anvil cells with their tiny sample chambers can be largely considered safe even in the Mbar range, while large-volume helium gas cells can be extremely dangerous at just a few bar of pressure. The danger is further enhanced if the energy of the compression is entirely transmitted to small parts (e.g. leads, windows), which can be propelled with high velocity. Best practice rules include (i) careful preliminary testing of the equipment before routine use, (ii) always working below ca. 90 % of the highest tested pressure value, (iii) changing pressure and/or temperature smoothly, (iv) using shielding and (v) depressurizing the cell immediately after taking the measurements [93].

2.1.1 Anvil Cells

Anvil cells, most commonly diamond anvil cells (DACs) have been used in scientific research for more than fifty years; having been continually modified and adapted to the specifications of a great range of characterisation and synthetic techniques, they still represent a relatively simple and safe way to obtain pressure up to the megabar range in the home laboratory [83]. Early iterations of the DAC comprised two opposing diamonds (supported by backing plates) between which a sample was compressed in a uniaxial manner. The use of gaskets in the DAC (shown schematically in Figure 3) allows for relatively hydrostatic environments by providing a chamber for the sample, which is filled with a hydrostatic medium that transmits pressure throughout the chamber. Perhaps the most significant influence on the actual pressure range attainable is the size of the smallest diamond face, or culet, with smaller culets able to produce significantly higher pressures [83]. The culet size of course also affects the size of the sample that may be studied in a DAC, with the largest samples often being no more than ≈ 300 μm in any one dimension and usually much smaller than this. It should be noted that for single crystal samples, the size must also be limited in the axial direction to avoid contact with both diamonds simultaneously, which would result in pressure gradients across the sample and, in the case of molecular materials, likely destruction of the crystal.

The diamonds are supported by seats and/or backing plates and pressure is generated by driving the diamonds together, deforming the gasket to reduce the volume of the sample chamber. Perhaps the simplest design for DACs is the Merril-Bassett DAC [94], shown schematically in Figure 3b, in which pressure is increased by manually by tightening screws in the cell body. Its simple design allows it to be relatively compact, enabling it to be easily incorporated into a variety of different experimental setups. This is vital in the field of SCO, where a combination of several experimental techniques (structural, spectroscopic etc) under the exact same conditions is often required to elucidate complex pressure effects. For example, a combination of high pressure single-crystal X-ray diffraction and Raman spectroscopy using the same DAC allowed for the rationalisation of complex pressure-induced SCO behaviour that differs significantly from the thermal behaviour in a dinuclear Fe(II) complex [80]. Another common design of DAC uses an inflatable gas membrane to apply pressure [95]. This latter method of pressure generation allows for finer control over the pressure at the sample via an external controller, and also allows for more controlled release of pressure if measurements as a function of decreasing pressure are of interest. This opens the possibility to study piezo-hysteresis loops of SCO materials, which may be difficult to investigate using screw-driven DACs. It should

however be noted that membrane-driven cells tend to be more complicated, more expensive and bulkier than screw-driven cells.
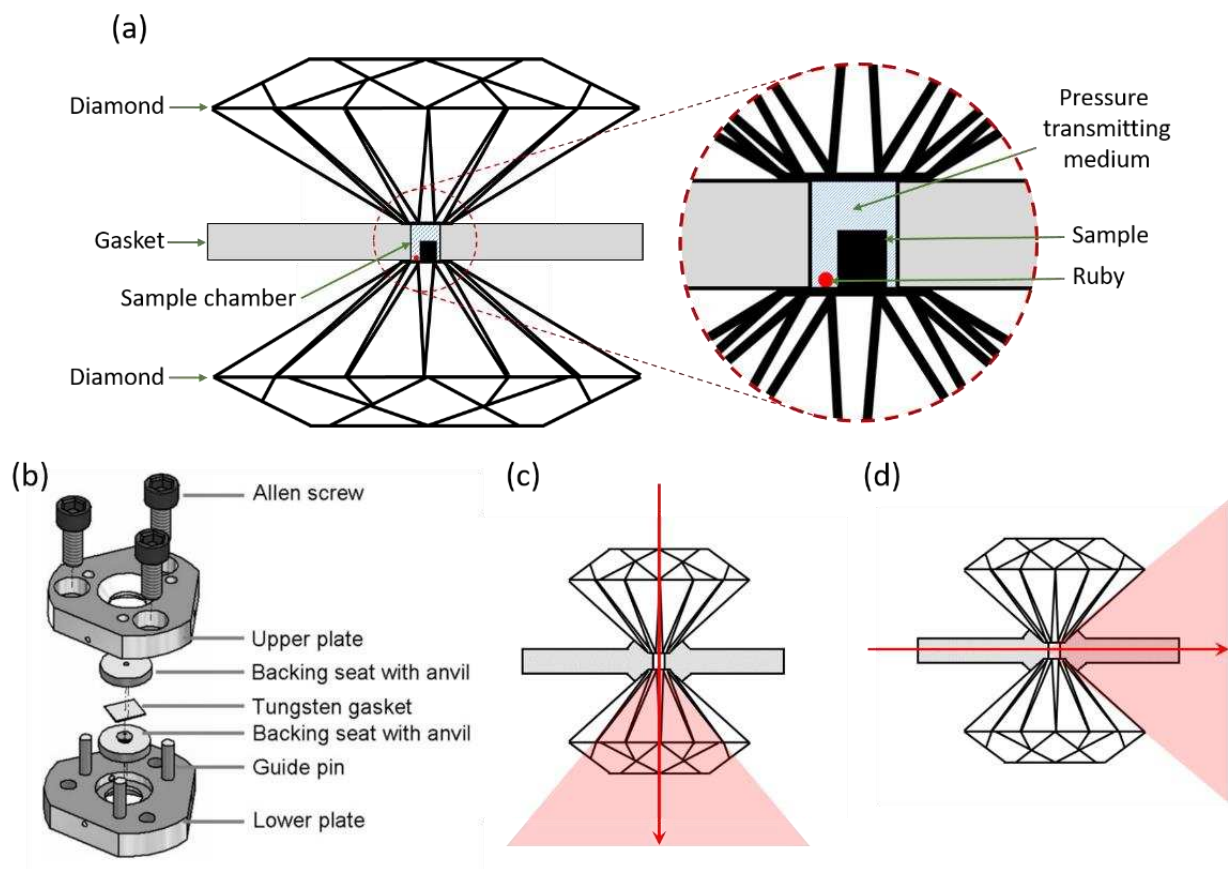

Figure 3. Diamond anvil cells (a) Schematic gasketed DAC, (b) exploded view of a Merrill-Bassett DAC as presented in [96]**, reproduced with permission of the International Union of Crystallography. Illustration of a DAC used in (c) transmission and (d) transverse geometry**

The simplicity and adaptability of the DAC design, coupled to the fact that the diamonds (depending on the type and level of impurities) are to a greater or lesser extent transparent to many types of radiation, have resulted in their use for a multitude of experimental techniques. The most relevant of these to the field of molecular SCO materials include X-ray and neutron diffraction, X-ray spectroscopy, Mössbauer spectroscopy, Raman, FTIR, UV-VIS and other optical spectroscopies. Two modes of use may be considered for the anvil cells: the probe radiation reaches the sample through the anvils which act as windows (either in transmission or reflection geometry); or the probe passes through the gasket to the sample – transverse geometry, as illustrated in Figure 3c and d. In general, transmission or reflection are the most commonly used DAC geometries when considering all experimental techniques, although some early examples of high pressure diffraction experiments used DACs in transverse geometry [76,97,98]. In that case a beryllium gasket provides the X-ray transparent sample chamber, as shown schematically in Figure 3d. The limiting factor to this design is the toxicity of the Be gasket material. The dangers associated with machining beryllium have largely resulted in its elimination from use as a gasket material, and thus transmission geometry cells becoming much more widely used. Other materials have been suggested as a replacement for Be [99], but none have yet found application in the study of molecular SCO materials. In transmission (or reflection) geometry the choice of material for the gasket is rather freer as it does not need to be transparent to the probe radiation. Many different metals have been used, with the commonest being stainless steel and rhenium. The choice is largely dictated by the pressure range of interest, with harder metals being required for the highest pressures. Gaskets can also be preindented before

making the hole for the sample chamber, which will considerably increase the pressure range achievable due to work-hardening the active region of the gasket and providing massive support [100]. For molecular-based SCO materials the pressure range of interest tends to be below 5 GPa, and thus stainless steel, used without preindenting is often sufficient. The advantage here is the possibility to drill gasket holes using standard – if small – drilling equipment without the need for accurate placement of the hole within the preindent. Such accurate placement can be done using a spark-eroder coupled to a microscope and x-y translation stage [101]. Generally the diameter of the hole that forms the sample chamber should be no more than 50% of the width of the culets, should be circular and strictly perpendicular to the plane of the gasket sheet to avoid pressure gradients. The gasket hole should also be well centred on the diamond culet. Imperfect or poorly centred gasket holes can lead to a blow-out of the sample chamber, loss of the sample and even destruction of the diamonds.

DACs built from non-magnetic materials have recently been adapted to fit within the confines of a SQUID magnetometer [102,103], increasing the potential pressure range available to magnetic studies beyond that offered by a piston-cylinder cell (*vide infra)* by an order of magnitude. It also allows the possibility of incorporating light irradiation into the high pressure experiment through the diamond windows, allowing observation of pressure-induced photomagnetic effects in SCO materials [104]. It is possible to use anvils other than diamond in these cells to reduce the cost of the equipment. Cubic zirconia, sapphire and moisonite anvils are commercially available, and can be employed for a range of experiments provided they are translucent to the probe radiation and are suitable for the pressure range of interest. It may also be worth mentioning that toroidal anvil [105] and multianvil [106] devices may provide an interesting, yet unexplored, scope for SCO research with considerable advantages in terms of larger sample volumes and more precise control of temperature and pressure fields.

2.1.2 Piston-cylinder type systems

Probably the most straightforward way to generate pressure is the use of piston-cylinder type systems, in which the cylinder acts as a pressure chamber and the piston is used to compress the medium. In particular these systems allow for accurate pressure determination on a force-per-area basis, provide hydrostatic conditions and large sample volumes. Despite the inherent opacity of the materials used to construct pistons and cylinders, windows for various probe radiations and electrical feedthroughs can be easily implemented. The latter are generally not used in the study of SCO materials, although they are required when calibrating the applied pressure. In general piston-cylinder cells can be used up to $1 - 4$ GPa, but the maximum pressure achievable is dependant largely on the size of the cell as well as the material from which the cell is constructed [107,108]. A key limiting factor is the yield-strength of the cylinder, which can be improved by different methods – the most popular being the autofrettage [93].

In the SCO field, clamped piston-cylinder cells are used preferentially in combination with magnetic and optical measurements. In this configuration, after applying a pressure with a press, the cell is clamped by locknut(s) to keep the piston(s) in the desired position – even after removing the cell from the press. These (relatively) small, autonomous cells are particularly popular because they can be easily combined with cryostats, magnetometers and other equipment [26,82,109]. While several designs, both home built and commercially available have been used in the study of SCO materials, the principle upon which they work is similar. In general the sample is placed in a Teflon capsule

along with a pressure-transmitting oil and, in some cases, with a Pb or Sn pressure gauge (*vide infra*). The sample capsule is placed inside the cell body and pressed by the pistons as shown in the cross-section in Figure 4. After clamping the cell, it is placed usually in a cryogenic flow and temperature cycles are carried out for a given pressure. Then, this operation is repeated while progressively increasing the pressure.
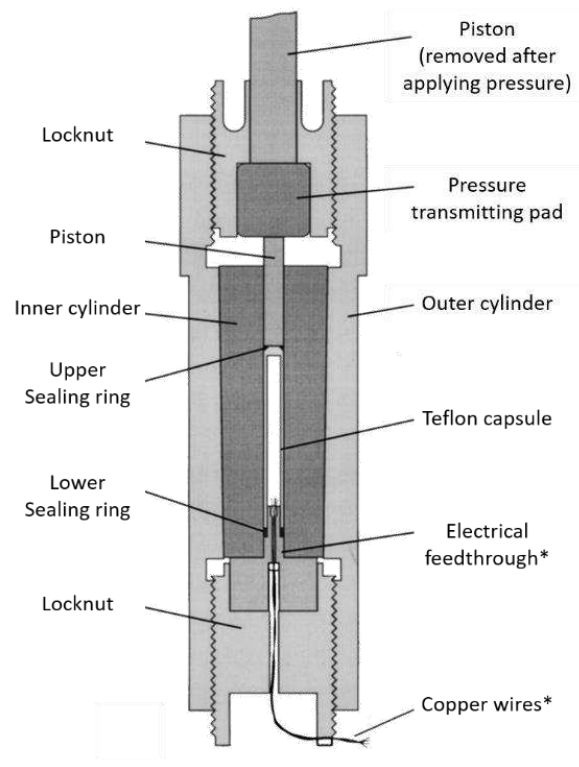

Figure 4. Cross-section of a typical clamp-type piston-cylinder pressure cell. Components marked * may only be used during pressure calibration. Reprinted from [108], with the permission of AIP Publishing

2.1.3 Capillary fed hydrostatic cells

While DAC and clamp type cells will no doubt remain popular for the ease of their use and their compact, autonomous construction, an important concern for SCO research is that they can potentially present difficulty when investigating isothermal pressure cycles (e.g. piezo-hysteresis effects). In addition, they are not readily designed for working at relatively low pressures (< 1 GPa) nor do they allow for a fine control of the pressure (partly for the lack of appropriate pressure gauges). Perhaps even more importantly, they exhibit an inevitable drop of pressure upon cooling. The freezing of the pressure transmitting oil may also lead to less hydrostatic conditions. Most of these drawbacks can be alleviated to some extent by gas loading and improved design (e.g. in membrane-driven DACs), but this inevitably brings in bulkier and much more complex instrumentation.

To overcome the limitations of DAC and clamp type cells one can also use a helium gas compressor or a liquid pump connected by a capillary to the pressure cell, an example of which is shown in Figure 5a. The pressure limit of these systems is usually limited by the capillary to a few kbar (< 1 GPa), the pressure generators are often rather complex and the potential danger of compressed gases is significant, yet they have allowed the investigation of unique features of the SCO phenomenon. A key advantage of this approach is that truly hydrostatic conditions can be maintained down to very low temperatures (using He gas). In addition one can increase/decrease both temperature and pressure in very

small increments (frequently < 0.005 GPa and < 1 K) in a facile manner, which provides a unique means to explore the P,T-phase diagram. This high precision is partly attributable to high precision valves and mechanical gauges (e.g. the Bourdon tube gauge) which can be used in conjunction with these cells. The relatively modest pressure range is not a real drawback for SCO research. On the contrary, such low pressures are very difficult to achieve using a DAC or a clamp cell and therefore these systems allow an important region of the structural phase diagram to be investigated. Last but not least, contrary to the above mentioned static pressure generators, these capillary systems combined with automatic valves can also allow for dynamic (e.g. pulses) pressure generation as well [110].

Capillary fed "low pressure" cells have been used with UV-vis spectroscopy (either in transmission or reflection mode), Mössbauer spectroscopy, Raman spectroscopy and dielectric measurements to investigate SCO compounds [25,49,60,111,112]. The first observation of a piezo-hysteresis effect used such a cell to investigate the SCO behaviour of the molecular $[Fe(btr)_2(NCS)_2] \cdot H_2O$ complex using optical reflectivity [77]. A simple pressure cell that uses a quartz capillary filled with nitrogen gas or water to generate pressures up to c.a 1 kbar in fine increments [113] was used to follow the structural evolution of a SCO material via single crystal X-ray diffraction [114,115]. This type of cell has advantages in that the pressures attained are close to those a material may be exposed to in real-world situations, and fine resolution of this important low pressure region is more accessible than with virtually any other technique.

A subsequent investigation used a cell driven by hydraulic oil pressure transmitting medium to investigate the SCO in a series of 3D coordination polymers using Raman spectroscopy [111]. Not only was it possible to observe a memory effect using a perturbation other than temperature, but the authors also used a theoretical analysis of their results to support their suggestion that piezo-hysteresis effects should be observed in many SCO materials. The importance of piezo-hysteresis loops has recently been highlighted for the ubiquitous $[Fe(Htrz)_2(trz)](BF_4)$ complex, which shows a pronounced pressure-induced increase in conductivity, as well as a significant piezo-resistive effect during SCO, as shown in Figure 5b-d [112]. These properties combined with piezo-hysteresis suggest that these materials may have a wealth of exciting possibilities in pressure sensing and piezoelectric applications.
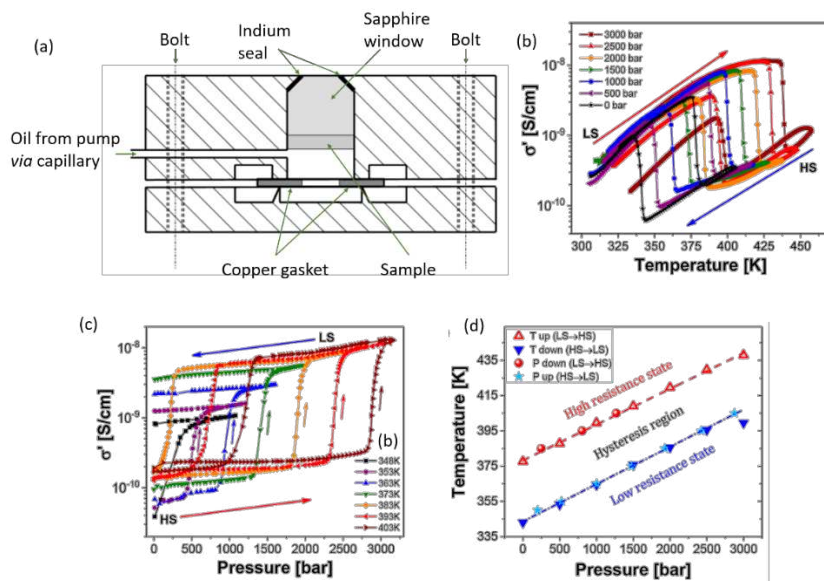

Figure 5. (a) Schematic of a capillary-fed hydrostatic cell, (b) temperature dependence of the electrical conductivity of [Fe(Htrz)₂(trz)](BF₄) at various applied pressures, (c) pressure dependence of the electrical conductivity of [Fe(Htrz)₂(trz)](BF₄) at various temperatures, and (d) the

2.2 Detection methods

In the second part of this section we discuss the different physical and spectroscopic methods used in conjunction with high pressure cells in the SCO field. For its recently growing importance as a readily available - though still highly specialized - laboratory technique with a key impact on the SCO field we discuss separately crystallographic techniques under pressure. Since magnetic susceptibility measurements remain a standard in the SCO field, we dedicate also a sub-section to high pressure magnetic methods. On the other hand, only a relatively brief account is given on the various other methods (Raman, FTIR, UV-VIS, Mössbauer and X-ray spectroscopies).

2.2.1. X-ray and Neutron Diffraction

There are relatively few high pressure structural studies of molecular spin crossover materials in the literature as highlighted by a recent review [116] perhaps as a result of the relative complexities of the diffraction experiment at high pressure when compared to ambient conditions or low temperature measurements. The relatively low pressure range of interest for molecular SCO materials means reasonably large single crystals can be investigated at high pressure inside DACs. As a consequence, standard diffraction equipment found in modern laboratories is suitable for high pressure single crystal diffraction experiments. However, in contrast to ambient pressure single crystal XRD experiments, experiments at high pressure require extensive user input and are still not considered routine. However, in recent years many diffractometer manufacturers include high pressure hardware options and specific software routines that can make high pressure data collection less challenging than even a few years ago.

Things which must be considered include the presence of additional Bragg reflections in the diffraction pattern from diamonds (and possibly ruby), angular dependant variation in transmission of X-rays through diamond, shadowing of the detector by the body of the DAC and the reduced access to reciprocal space due to the restricted opening angle of the DAC [117,118]. The vast majority of molecular crystalline materials (including SCO systems) have relatively low symmetry, most commonly crystallising in triclinic, monoclinic or orthorhombic space groups [119]. This means that single crystal diffraction experiments of such materials at high pressure are often incomplete and/or have low redundancy, as a result of the restricted access to reciprocal space imposed by the body of the cell [118]. This problem has in the past been mitigated by using an X-ray translucent berylium gasket and a transverse DAC geometry [120], shown schematically in Figure 1d. Rotation of the cell about the axis of the diamonds through 360° makes it possible to sample a much larger portion of reciprocal space than in transmission geometry. If the crystal is carefully oriented within the cell, a virtually complete unique dataset can be expected for monoclinic systems. This geometry was used in the first high pressure X-ray diffraction study of molecular SCO materials $Fe(phen)_2(NCS)_2$ and $Fe(btz)_2(NCS)_2$ [68] as well as in the study of SCO in the $[Mn^{II}(pyrol)_3tren]$ [78]. As described above, the dangers associated with machining beryllium have largely resulted in cells of transmission geometry becoming much more widely used in X-ray diffraction. Problems with low completeness in transmission geometry can be to some extent ameliorated by using more than one crystal in the sample chamber (each with different orientations) [121] or using short wavelength X-rays, for example at a synchrotron source. Modern transmission geometry DACs specifically designed for X-ray diffraction work

have opening angles of up to 100° thanks to careful design of the diamond anvils and backing plates [96]. Although complete datasets for monoclinic systems often still proves illusive, sufficient data can be collected to reliably investigate structural changes that occur on SCO, as confirmed by several complimentary experimental techniques[79]. For the lowest symmetry triclinic systems, it is often not possible to obtain anything more detailed than unit cell parameters as a function of pressure. While less information is gained in this case, unit cell parameters can still prove very informative for obtaining the volumic and axial compressibilities and thus rationalising elastic interactions and anisotropic lattice distortions.

The limitation of the sample size as well as the restricted angular aperture means that synchrotron radiation is almost always necessary to observe diffraction from powder samples inside DACs, where high-flux short-wavelength X-ray beams are available. However, with the increasing availability of Ag and Mo microfocus X-ray sources it may well be the case that high pressure powder studies become accessible outside of central facilities in the next few years.

Another challenge in high pressure structural studies of SCO materials is the combination of high pressure and variable temperature experimental environments. The vital importance of structural studies in rationalising SCO behaviour is clear, however, the difficulties associated with mounting a traditional DAC inside a cryostat on a goniometer have so-far limited such studies to central facilities [79]. Recent developments in the production of miniature DACs that can be mounted on an in-house diffractometer and are small enough to be cooled by standard open-flow cryo-cooling devices present exciting opportunities, [122] and it is hoped that such devices will accelerate research in this area.

The inherent low-flux of neutron sources, combined with the relatively low neutron scattering efficiency of materials, requires that larger sample volumes be used during neutron diffraction experiments. In the study of SCO materials this has been achieved using a TiZr clamp cell for high pressure neutron powder diffraction experiments [123,124].

2.2.2 Magnetic measurements

High pressure cells designed for use inside a superconducting quantum interference device (SQUID) magnetometer are limited in their design by the restrictions of the sample space and must of course be constructed from suitable materials. Both commercial and home-made clamp cells designed for magnetometry measurements have traditionally been constructed from beryllium bronze (CuBe) due to its high strength, good thermal conductivity and diamagnetic nature. It may be heat treated for increased strength, but it presents some potential dangers associated with toxic dust generated during machining of beryllium alloys. Beyond these considerations as to construction material, a pressure cell designed for use in a commercial squid magnetometer must also have a narrow diameter (typically 9mm or less) to fit within the bore of the sample chamber, and should be approximately symmetrical laterally over several cm, to aid with peak fitting and sample centring. The additional weight of the cell compared to standard (ambient pressure) measurements makes thoroughly securing it to the sample transport rod particularly important.

Pressure is applied using a hydraulic press via a piston that is removed after applying the desired pressure. To achieve a specific pressure at the sample, it is necessary to calibrate the pressure applied at the hydraulic press with that obtained in the cell using a four-wire measurement first using a manganin resistance gauge [93]. The pressure inside the cell is determined at very low temperatures by measuring the temperature of the superconducting transition of a small piece of either high purity Pb, In or Sn metal placed with the sample inside the sample capsule, as illustrated in

Figure 2. This calibration is done usually at very low temperature scan rates and by applying only a weak AC field due to the sensitivity of the superconducting transition to magnetic fields. It is important to note also that pressure will inevitably vary as a function of temperature due to thermal contraction of the cell and the pressure-transmitting oil. The pressure drop between room temperature and liquid helium temperature can be as high as 0.1-0.2 GPa.

The high pressure SQUID magnetometry experiment may be complicated by the large diamagnetic contribution of the cell body, Teflon capsule and pressure-transmitting oil. As a possible consequence, in the course of the temperature scan the magnetization may change between positive and negative values resulting to unacceptably poor fit for values close to zero magnetization. Adding a known quantity of a stable paramagnetic substance may resolve this issue. It is also sometimes unavoidable in a high pressure experiment that the sample mass is not accurately known. As such, calculating accurate values of $\chi_M T$ can be difficult; calculation of $\chi_M T$ may require the use of a series of calibration measurements in the absence of sample, and/or the application of a series of assumptions. Such assumptions may include that $\chi_M T$ of the sample in (e.g.) the HS state is equal to that observed in the HS state at ambient pressure, that that diamagnetic contribution is constant at all temperatures and that $\chi_M T$ of the sample is constant at temperatures well away from the SCO. It is important that the validity of any such assumptions is evaluated in each case before application. Since the first report of high pressure magnetic susceptibility measurements of SCO solutions [12] and solids [26], there have been numerous studies of SCO materials under pressure using SQUID magnetometry, which will be largely covered in section 3 of this review. There are also some reports of DACs that have been optimised for use in squid magnetometers [103]. As discussed previously, they have the potential to reach significantly higher pressures than clamp-type cells, but the small sample volume required by these cells has so-far limited their application to the field of molecular SCO. They do however present interesting possibilities for the incorporation of light irradiation, pressure and temperature within a single experiment.

2.2.3. Other detection methods

Since the SCO phenomenon is accompanied by the change of various material properties (electronic, structural, vibrational, magnetic, optical, electrical, etc.) it is not surprising that a large variety of detection methods have been used for its investigation under high pressures. Here we briefly review the most important ones.

High pressure Raman spectroscopy of SCO materials was first reported using the hydrostatic cell presented in Figure 5a [111], and has since been used several times as a straightforward means to follow the HS $\rightarrow$ LS transition as a function of pressure using characteristic marker bands for each state, [79,80,115,125–127], an example of which is shown in Figure 6. Specific marker of the two spin states can be first identified during a separate variable temperature experiment. Besides following the spin-state changes, in certain compounds Raman spectroscopy allowed to detect the occurrence of simultaneous pressure induced structural changes [111] and also to estimate the pressure induced modification of the vibrational entropy as inferred from the frequency shifts [88]. Raman spectroscopy has the advantage that it can operate at long working distances from the sample, allowing for the relatively bulky sample environment of a pressure cell. It can be used to probe small sample volumes often encountered in pressure cells, and the Raman spectrometer can be used to measure the pressure *via* the ruby fluorescence technique *in situ*. It can also be used to carry out complementary optical absorption measurements. Importantly, Raman spectroscopy can be

used to study single crystals, powders, thin films or solutions with virtually no sample preparation. Using reflection geometry, the only requirements for pressure cells used in Raman studies is that they have one window that is transparent to the wavelengths relevant to the experiment. Examples might include diamond, sapphire and quartz, although the use of DACs is perhaps the most common and convenient. When diamond is used as the window materials, the type of diamond needs to be selected carefully due to different fluorescence responses between type I and type II diamonds [128]. It is also interesting to note that laser-induced heating of the sample is reduced to a large extent in the high pressure cell (vs. ambient air) due to the improved heat dissipation provided by the pressure transmitting medium. This feature is obviously very advantageous in investigating SCO compounds.

Despite very early applications of the DAC in high pressure IR spectroscopy [83], the technique is complicated by the necessity for more expensive nitrogen-free diamonds, the small sample size, and requires specialised focusing optics to obtain a suitable signal-to-noise ratio [129]. While specific modifications to the DAC have been proposed to facilitate IR measurements [129] and FTIR microscopes have been also significantly improved recently, it is still not a routine experiment. While several high pressure IR spectroscopic studies of spin crossover materials using a DAC have been reported in the 70-80's [3,4,13–17,19,20,32] by now this technique has been largely replaced by high pressure Raman spectroscopy, giving access to similar information about the sample, while providing ease of use, no sample preparation and a larger selection of possible pressure transmitting fluids. Indeed, since the pressure-transmitting medium should not interfere with the spectrum of the sample, in the far-IR Nujol is often used, but the relatively low hydrostatic limit of Nujol limits the investigated pressure range to below 1.5 GPa [32].
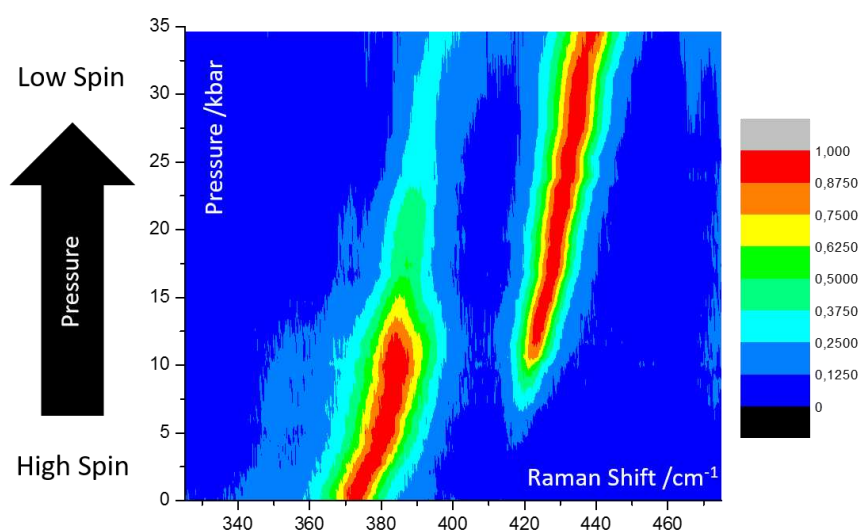

Figure 6. Normalised Raman intensities of characteristic marker peaks of a molecular spin crossover material at 370 (HS) and 420 cm^{-1} (LS) as a function of pressure, adapted from [80]

A significant number of high pressure ^{57}Fe Mössbauer spectroscopic investigations of SCO materials were reported and reviewed several years ago [82]. The key interest of this technique that it usually allows for a simple, yet accurate quantification of the high spin fraction as a function of pressure and temperature in iron complexes. In general, either clamp-type or capillary-fed cells were used, incorporating windows that are transparent to gamma radiation, most commonly boron carbide [25,130]. (N.B. Beryllium is a more suitable window material, but it is scarcely used due to its previously mentioned toxicity.) Pressure transmitting media include inert gasses and oils. In general, studies consist of variable temperature investigations at high pressure, and as such represent one of the few early examples of

combining more than one external stimulus to control the spin state in these materials. One significant limitation of this technique is the relatively small sample volume often encountered in high pressure cells. This fact, combined with the relatively small Fe content and low Lamb-Mössbauer factor of typical SCO samples as well as with the restricted γ-ray transmission of the windows makes isotope enrichment of the samples with ^{57}Fe to give a suitable signal-to-noise ratio inevitable [82]. For this reason, high pressure Mössbauer spectroscopy has been sparingly used in the study of molecular SCO materials in recent years. Sample volume is even more restricted in DAC-type cells used in conjunction with Mössbauer spectroscopy. In this case, not only isotope enrichment, but also high specific-activity, 'point' sources have been employed [23]. However, these sources imply increasing linewidths and increasing price. DACs can be advantageously used in combination with synchrotron radiation sources. Notably, nuclear inelastic scattering (NIS) experiments at pressures up to 2.6 GPa has been performed for two powder samples of molecular SCO complexes [131]. The pressure cell was based on a DAC design, but was adapted to the requirements of the technique by incorporating photodiode detectors close to the sample chamber to detect nuclear fluorescence signals. The study enabled the determination of the partial vibrational density of states for the complexes as a function of pressure for the first time, revealing similar changes to those occurring as a function of temperature.

Synchrotron X-ray spectroscopy techniques, such as X-ray absorption near edge structure (XANES), extended X-ray absorption fine structure (EXAFS), X-ray emission (XES), X-ray magnetic circular dichroism (XMCD), etc, are particularly well-suited for the investigation of SCO complexes under pressure as they allow to probe the spin-state quantitatively in small sample volumes with elemental sensitivity. Indeed, the first high pressure XANES studies of SCO complexes investigated the phenomenon in both Co^{2+} [70] and Fe^{2+} [66] complexes using a DAC. Interestingly, in both cases, the authors reported significant shifts in the pressure required to switch between HS and LS states on repeated cycling. This effect was subsequently attributed to the reduction in the number of defects in the lattice on pressure-cycling. Similar effects are commonly observed on thermal SCO, and so perhaps it should not be surprising that observations should also be made with pressure. That this effect has not been observed more frequently on pressure-cycling is perhaps just a result of the rarity of experiments that repeatedly cycle the same sample with pressure. Subsequent XANES studies allowed not only to establish the high spin fraction vs. pressure curves, but also to follow the main structural changes using EXAFS [43][61]. As a final note on synchrotron X-ray experiments it may be worth noting that the intense, focused X-ray beam may lead to the degradation of relatively fragile SCO complexes and therefore the sample integrity must be always carefully controlled. (N. B. The same concern applies to laser Raman spectroscopy.)

High pressure optical (UV-VIS-NIR) absorption measurements on single crystals and solutions as well as reflectivity measurements on powder samples represent simple and efficient means to probe the SCO phenomenon through the piezo-chromic properties of spin crossover complexes. In particular, quantitative optical absorption measurements on crystals can be carried out using a cheap optical microscope and an appropriate bandpass filter. Optical spectroscopy has been used since the onset of SCO research [10,11,16,49,59,132] in conjunction with DACs, piston-cylinder and capillary-fed cells as well. Optical spectroscopy is particularly well suited for time resolved measurements. For instance, McGarvey et al. [33] used pulsed-laser photoperturbation technique together with a capillary-fed cell to determine both the reaction and activation volumes of various SCO complexes in solution. Solid samples were also investigated by Hauser et al. [57] using pump-probe optical spectroscopy in combination with DAC and an impressive,

eight orders of magnitude acceleration of the low-temperature tunnelling process could be evidenced for an external pressure of 2 GPa. We expect that recent ultrafast (fs) optical spectroscopy experiments on SCO samples will be also complemented by measurements under pressure in the near future.

3. Pressure effect studies on Fe(II) spin crossover or paramagnetic coordination compounds

As described in the introduction, the effect of pressure on SCO compounds is to stabilise the LS state due to its smaller ionic radius (ca. 0.2 Å smaller in LS than HS state for Fe(II) complexes). The change of volume provides the driving energy in pressure induced phase transitions $[(\partial G/\partial p)T = V]$. For most of the SCO complexes investigated, the transition/equilibrium temperature (usually denoted $T_{1/2}$) of the SCO is shifted upwards with increasing pressures, and the hysteresis width and steepness (cooperativity) of the SCO decrease and vanish at a critical pressure [82]. However, there are a significant number of examples of SCO compounds where the shape of the SCO curve remains essentially unaltered across a reasonable range of pressure, the hysteresis increases/decreases or nonlinear behavior of the $T_c(p)$ versus p plot is exhibited [47,50,54,133–135]. In rare cases stabilization of the HS state under pressure has also been reported [134]. From a phenomenological viewpoint, these different behaviours seem to depend on the change of the elastic energy of the material (compressibility) and the intermolecular interactions in the crystal under pressure [136]. Structural features including hydrogen bonding, π-π stacking or metallophilic interactions will be affected differently by pressure, and are not distributed isotropically throughout the material. As such the structural changes induced by the application of pressure may be highly anisotropic, affecting the total volume change during the HS $\leftrightarrow$ LS transition [116]. Theoretical progress in understanding such unexpected pressure effects requires systematic investigations on single-crystal structure determination under applied pressure to rationalise the origin of unusual pressure-induced SCO behaviour on a case-by-case basis [68,79,80,98,116,123,127].

3.1 Compounds undergoing continuous thermal spin crossover

For a continuous – or gradual – thermal spin conversions without hysteresis, most materials behave as predicted by the Clasius-Clapyron equation as described in the introduction. In general, application of hydrostatic pressure results in stabilization of the LS state and a concomitant shift of the transition temperature upwards. Examples of such behaviour are presented in Table 1 [22,53,137–143], along with the change in their $T_{1/2}$ values as a function of pressure. The compound [Fe(H$_2$B(pz)$_2$)$_2$(bipy)] [134] is a representative example of such type of pressure-induced behaviour, and is shown in Figure 7, along with $\chi_M T$ versus T curves (χ_M is the molar magnetic susceptibility, and T the temperature) at different hydrostatic pressures. At atmospheric pressure, $T_{1/2}$ is 160 K and the transition is complete within 70 K. Between 0.2 and 0.5 GPa the spin transition experiences a shift to higher temperature and its character become more continuous. Indeed, under pressure the SCO becomes more gradual, occurring over a range of more than 150 K at 0.5 GPa. The variation in $T_{1/2}$ is linear as a function of pressure: 210 K (0.26 GPa), 233 K (0.4 GPa) and 255 K (0.5 GPa). The slope of the line in the $T_{1/2}$ vs P plot, $dT_{1/2}/dP$ = 187.5 K GPa^{-1} is comparable with the values observed for several mononuclear compounds whose magnetic properties under pressure have been investigated (Table 1). As well as

these molecular complexes with continuous SCO behaviour, the coordination polymers [Fe(3py-im)$_2$(NCS)$_2$]·7H$_2$O [142] and [Fe(dpms)$_2$(NCS)$_2$] [143] also show typical pressure-dependant magnetic properties.
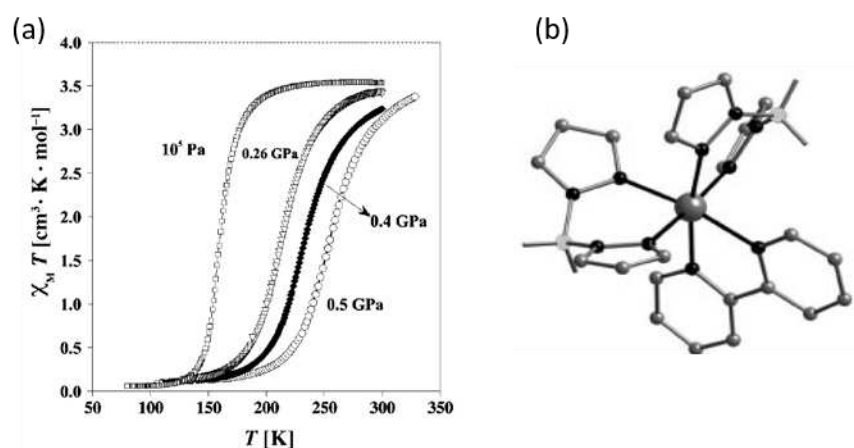

Figure 7. (a) Magnetic properties under hydrostatic pressure in the form of χ_MT vs T and (b) illustration of the molecular structure of the complex [Fe(H$_2$B(pz)$_2$)$_2$(bipy)]. Reproduced with permission from [134]**.**

Table 1. Values of d$T_{1/2}$/dP in K GPa^{-1} for Fe(II) mononuclear coordination complexes exhibiting continuous thermal spin conversion.

Compound	d$T_{1/2}$/dP in K GPa^{-1}
[Fe(pmea)$_2$(NCS)$_2$] [140]	146
[Fe(pic)$_3$]Cl$_2$·EtOH [22]	150
[Fe(PM-AzA)$_2$(NCS)$_2$] [53]	160
[Fe(dpa)$_2$(NCS)$_2$] [138]	176
[Fe(abpt)$_2$(NCS)$_2$] polymorph I [139]	176
[Fe(stpy)$_4$(NCBH$_3$)$_2$]trans [141]	186.3
[Fe(H$_2$B(pz)$_2$)$_2$(bipy)] [134]	187.5
[Fe(phen)$_2$(NCS)$_2$] polymorph II [137]	220

3.2 Compounds with abrupt thermal spin transition accompanied with hysteresis

Again, many compounds with abrupt spin transitions at ambient pressure also show typical pressure-induced SCO behaviour. [Fe(2-pic-ND$_2$)$_3$]Cl$_2$·EtOD [144] and [Fe(bt)$_2$(NCS)$_2$] [67] are typical examples, where the transition temperature increases and the hysteresis and the slope of the transition curve diminish as pressure increases. The hysteresis vanishes at a critical pressure, and at even higher pressures the transition transforms to the gradual type. More unusual behaviour has been displayed by the complex [Fe(phy)$_2$](BF$_4$)$_2$, which shows an increase of the width of the hysteresis loop under pressure, as depicted in Figure 8. In addition, a nonlinear response of $T_{1/2}$ as a function of pressure has been reported. This singular behaviour was explained using the mean field theory by introducing the dependence of the bulk modulus (K) under pressure [50]. However, to date there is no single crystal diffraction data at high pressure to further probe this unexpected behaviour.
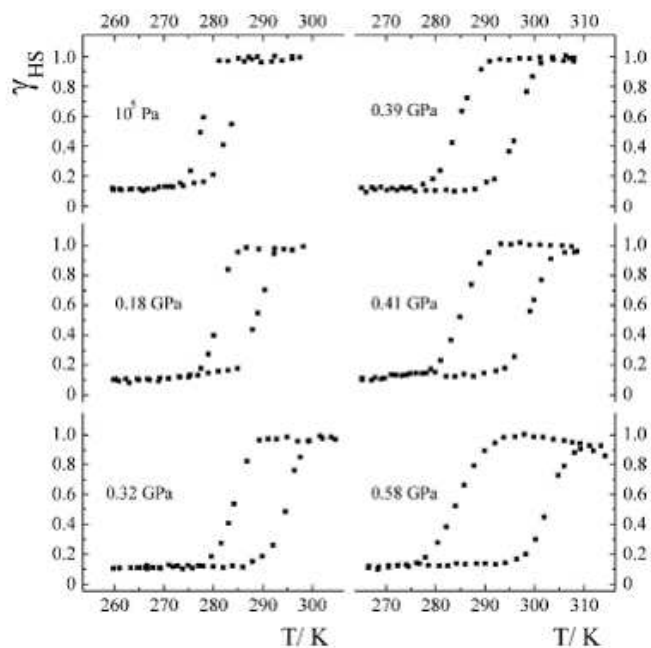
Figure 8. Plot of γ_{HS} vs. *T* , high spin molar fraction versus temperature, at different pressures for [Fe(phy)$_2$](BF$_4$)$_2$. Reprinted from [50] **Copyright (1999) with permission from Elsevier.**

A series of mononuclear complexes of general formula [Fe(PM-L)$_2$(NCS)$_2$] (where PM-L ligands represent a series of 2 -pyridylmethylene 4-anilino derivatives) were studied under pressure [53] and revealed a variety of different behaviours, including increasing width of hysteresis in [Fe(PM-BIA)$_2$(NCS)$_2$]. Subsequent high pressure reflectivity [145] and neutron diffraction structural studies [124] allowed the complex interplay between polymorphism, phase transitions and SCO effects to be assessed in detail. Other unusual effects seen in this class of compounds includes irreversible increases in hysteresis width after pressure is released in [Fe(PM-PEA)$_2$(NCS)$_2$] [53]. While detailed structural investigation of this material as a function of pressure was prevented by reduction of crystal quality [114], a phase transition under pressure was clearly demonstrated. Such pressure-induced irreversible modification may well represent an interesting method for tuning properties of SCO materials, and as such, the importance of measuring the properties of the material under ambient conditions after depressurisation is clearly highlighted.

A study of the compound [Fe(dpp)$_2$(NCS)$_2$]·py (dpp = dipyrido[3,2-a:2'3'-c]phenazine and py = pyridine) highlights clearly the importance of high pressure structural studies in understanding unusual pressure-induced behaviour, and even sheds light on the mechanism of the thermal transition responsible for the highly cooperative thermal SCO behaviour. At ambient pressure it displays a very cooperative spin transition with a 40 K hysteresis width, accompanied by an isostructural crystallographic phase transition. High pressure structural studies revealed a highly anisotropic scissor-like distortion of the molecule (Figure 9) coupled to physical intercalation of the large dpp ligands as the origin of the highly cooperative interactions observed [127]. The mechanism is also responsible for exotic mechanical behaviour including negative thermal expansion and negative linear contraction. The ability of the lattice to accommodate the opposing change in shape of the molecule during the spin transition is what governs whether or not the HS-LS transition can occur. This is essentially an elastic property of the lattice; as the volume of the HS cell contracts by 2% on cooling from 275 to 150 K, the lattice can accommodate the change in shape required for SCO to occur. The same contraction, but with a much greater magnitude (15%) occurs on pressurization up to 0.18 GPa and

the lattice is no longer capable of accommodating the change in geometry. The HS-LS transition is thus suppressed, but eventually under the application of further pressure a spin transition occurs to a structurally distinct LS state.
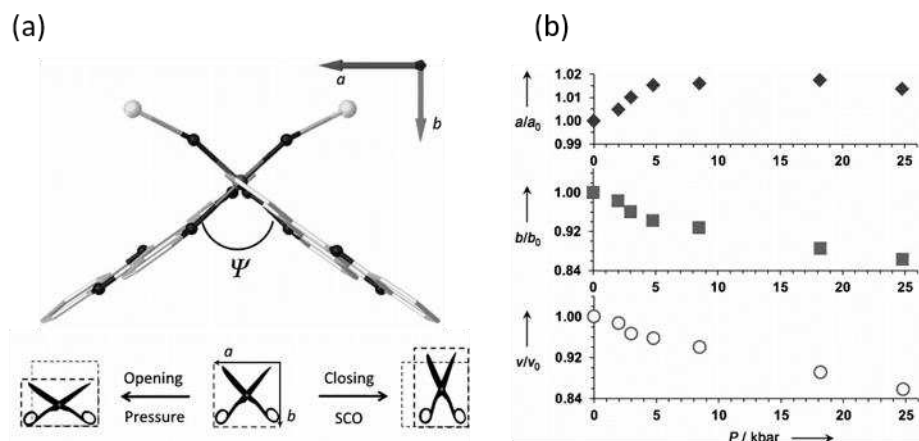

Figure 9. (a) Structure of the molecule [Fe(dpp)$_2$(NCS)$_2$]·py in the *ab* plane denoting the relative orientation to the unit cell axes. The Ψ angle quantifies at the molecular level the "scissor-like opening-closing" mechanism that induces or inhibits the spin crossover process. The *a* and *b* axes change as a consequence of the opening (HS) or closing (SCO) mechanism. (b) Variation of the *a* and *b* axes together with the cell volume as a function of pressure derived from single-crystal diffraction studies. Reproduced with permission from [127]

In addition to molecular complexes, several coordination complexes have also shown interesting behaviour under pressure. For example, the 3D coordination complex {Fe(pmd)(H$_2$O)[Ag(CN)$_2$]$_2$}·H$_2$O [133], shows pressure-tunable thermal bistability as well as piezochromic bistability at room temperature. Figure 10 shows the polymeric structure, the $\chi_M T$ vs. *T* curves at different pressures and the pressure dependence of the high-spin molar fraction at room temperature. In the crystal there are two different iron(II) pseudo-octahedral sites, [FeN$_6$] and [FeN$_4$O$_2$]. The equatorial positions of both sites are occupied by the nitrogen atoms belonging to the [Ag(CN)$_2$]$^-$ anions, while the axial positions are occupied by pmd ligands and water molecules, respectively. The [Ag(CN)$_2$]$^-$ ligands act as bridges connecting both sites defining an infinite 3D open framework. Three identical nets interpenetrate to fill the empty spaces. As evidenced by the $\chi_M T$ vs. *T* plot pressure allows one to place the hysteresis loop at will in a large range of temperatures without losing its well defined square shape. At 300 K, the electronic spectrum in the visible region acquired at different pressures demonstrate that the compound undergoes a complete pressure-induced SCO accompanied by reproducible piezohysteresis loop of 0.2 GPa. The transition pressure values corresponding to half-conversion are $P^{up}_c \approx 0.71$ GPa and $P^{down}_c \approx 0.52$ GPa.
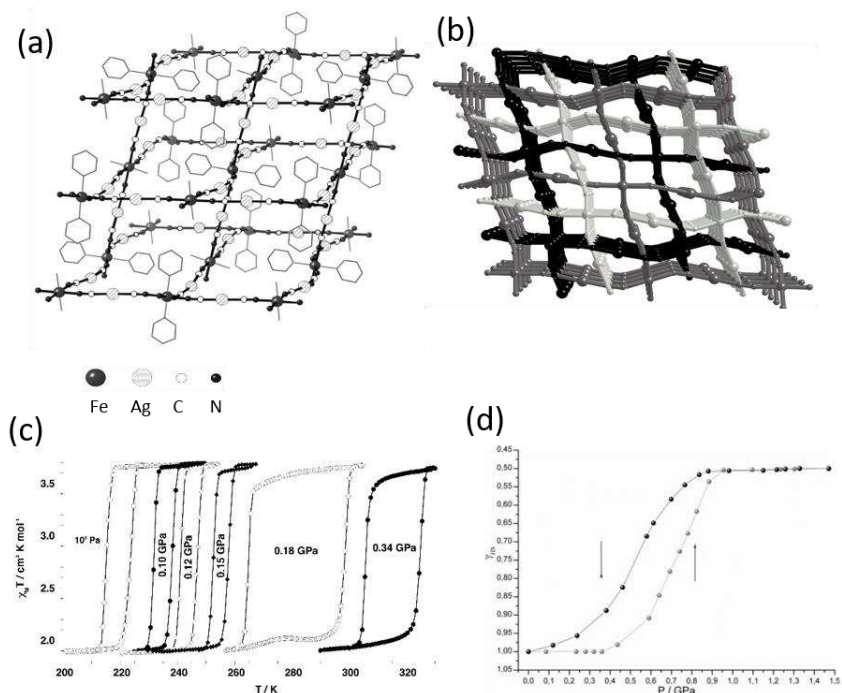
Figure 10. (a) Picture of the 3D network and **(b)** perspective view of the three interlocked networks of {Fe(pmd)(H$_2$O)[Ag(CN)$_2$]$_2$}·H$_2$O. **(c)** $\chi_M T$ vs. T curves at different pressures for {Fe(pmd)(H$_2$O)[Ag(CN)$_2$]$_2$}·H$_2$O: 10^5 Pa, 0.10 GPa, 0.12 GPa, 0.15 GPa, 0.18 GPa and 0.34 GPa. **(d)** Pressure dependence of the high-spin molar fraction, γ_{HS}, of the spin crossover iron(II) ions at 300 K deduced from the visible spectra. Reproduced with permission from [133].

Other Fe(II) 2D coordination polymers investigated include {Fe(3-F-py)$_2$[M(CN)$_4$]} [132,135] (M(II) = Ni, Pd and Pt), {Fe(3-Cl-py)$_2$[Pd(CN)$_4$]} [146] and {Fe(phpy)$_2$[Ni(CN)$_4$]} [147]. The main structural difference among the 2D polymers based on 3-X-pyridine ligands and that based on the ligand 4-phenylpyridine is the distance between the {Fe[M(CN)$_4$]}$_\infty$ layers imposed by the organic ligand and the strength of the π–π contacts. Table 2 gathers characteristic transition pressures derived from spectroscopic experiments in the visible region at 298 K carried out for these complexes. The compound {Fe(phpy)$_2$[Ni(CN)$_4$]} presents the largest inter-sheet distance as well as the largest Δp$_c$ observed (0.3 GPa). Presumably, compound {Fe(phpy)$_2$[Ni(CN)$_4$]} acts as a better pressure absorber than the above-mentioned 3D and 2D cyanide-based SCO polymers. Recently, a theoretical study has demonstrated that the changes of the elastic and inelastic forces in the crystal as a function of pressure or temperature determine the behaviour of the spin transition in these polymers [132,148].

Table 2. Characteristic transition pressures derived from visible spectroscopic experiments at 298 K for several cyanide based Fe(II) spin crossover coordination polymers

Compound	$p_c^{\uparrow}$, GPa	$p_c^{\downarrow}$, GPa	p_c^{av}, GPa	Δp_c, GPa
{Fe(pmd)(H$_2$O)[Ag(CN)$_2$]$_2$}·H$_2$O [22]	0.71	0.52	0.615	0.2
{Fe(3-F-py)$_2$[Ni(CN)$_4$]} [53,140]	0.38	0.29	0.33	0.1
{Fe(3-F-py)$_2$[Pd(CN)$_4$]} [53,140]	0.39	0.27	0.33	0.11

{Fe(3-F-py)$_2$[Pt(CN)$_4$]} [53,140]	0.34	0.27	0.30	0.07
{Fe(3-Cl-py)$_2$[Pd(CN)$_4$]} [141]	0.65	0.57	0.61	0.08
{Fe(phpy)$_2$[Ni(CN)$_4$]} [142]	1.6	1.3	1.45	0.3

3.3. Compounds with multi-stepped spin transitions

Multi-stepped spin transitions are those spin transitions with two or more discernible steps (gradual or abrupt) separated by plateaus or discontinuities along the γ_{HS}(T) curve (γ_{HS} = high spin molar fraction). A two-step spin transition was first observed in the mononuclear compound [Fe(2-pic)$_3$]Cl$_2$·EtOH [22]. Later on the same phenomenology was reported for dinuclear coordination complexes [149,150] as well as for a series of Fe(II) polymeric species [151–153]. Recently, three- and four-step spin transitions have been reported for both polynuclear [154,155] and polymeric Fe(II) compounds [156]. Examples of multi-stepped SCO in Fe(III) coordination compounds are scarce [157]. Detailed variable-temperature crystal structure analysis in conjunction with magnetic, calorimetric and spectroscopic studies revealed that the short- and long range elastic interactions in the crystal lattice are responsible for the energetic stabilization of the [···HS-LS···] "chessboard" structures. Thus, step like SCO behaviour can arise as a consequence of the elastic forces in the crystal [158–165]. Alternatively, multistepped spin transition can also be observed when two or more chemically or crystallographically non-equivalent iron centres are present either in the crystal lattice or in a cluster. In such a case, each iron centre undergoes spin transition at different temperature, resulting in a stepwise spin transition [135,166]. Pressure provides a unique tool to probe elastic interactions in the solid state, and as such have been used to examine complexes showing stepped SCO behaviour.

Dinuclear complexes based on the 2,2′-bipyrimidine bridge ligand (bpm), {[Fe(bpm)(NCSe)$_2$]$_2$bpm} and {[Fe(bt)(NCX)$_2$]$_2$bpm} (X: S, Se and bt : 2,2`-bithiazoline), show one-step [HS–HS] $\leftrightarrow$ [HS–LS] and two-step [HS–HS] $\leftrightarrow$ [HS–LS] $\leftrightarrow$ [LS–LS] spin transitions, at atmospheric pressures, respectively. Figure 11 shows the magnetic properties under applied hydrostatic pressures in the form of χ_MT vs T [73]. At 0.45 GPa, {[Fe(bpm)(NCSe)$_2$]$_2$bpm} undergoes less steep [HS–HS] $\leftrightarrow$ [HS–LS] conversion and the transition temperature is shifted upwards. As pressure increases the SCO curve transforms into a two-step curve, which is complete at 1.03 GPa. The plateau between the steps smears out and diminishes as the pressure increases. The magnetic behaviour of {[Fe(bpm)(NCSe)$_2$]$_2$bpm} under pressure resembles that of the dinuclear complexe {[Fe(bt)(NCX)$_2$]$_2$bpm} at atmospheric pressure. For compound {[Fe(bt)(NCSe)$_2$]$_2$bpm} the spin transition is displaced 50 K at relatively low pressures (0.37 GPa) [73].
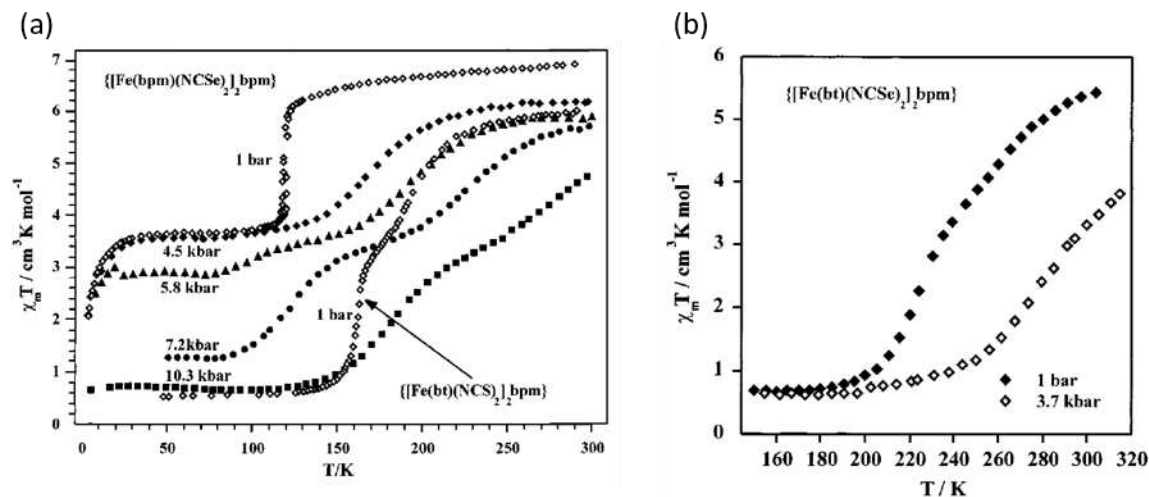
Figure 11. (a) Temperature dependence of $\chi_M T$ for {[Fe(bt)(NCS)$_2$]$_2$bpm} at atmospheric pressure and for {[Fe(bpm)(NCSe)$_2$]$_2$bpm} under applied hydrostatic pressure. (b) Temperature dependence of $\chi_M T$ for {[Fe(bt)(NCSe)$_2$]$_2$bpm} under applied hydrostatic pressure. Reprinted with permission from [73]. Copyright (2001) American Chemical Society.

In contrast to the magnetic behaviour of bpm-based dinuclear complexes under pressure, the dinuclear complex [Fe$_2$(PMAT)$_2$](BF$_4$)$_4$·DMF shows only one step [HS–HS] $\leftrightarrow$ [HS–LS] spin transition up to 1.03 GPa [167]. The steepness of the transition observed at 10^{-4} GPa disappears gradually as pressure increases. The inhibition of the spin conversion in the second iron centre of the dinuclear unit seems to be related to the steric constrains imposed by the bridge ligand.

Another dinuclear complex undergoing a steep one step spin transition at 10^{-4} GPa is [Fe(bpp)(NCS)$_2$}$_2$(4,4$'$-bipy)]·2MeOH (bpp = 2,6-bis(pyrazol-3-yl)pyridine and 4,4'-bipy = 4,4'-bipyridine) [80]. In this compound it has been not possible to elucidate if the one step spin transition observed at 10^{-4} GPa corresponds to [HS–LS] molecules or a random distribution of 50% [HS–HS] and [LS–LS] dinuclear units in the crystal lattice. Raman and structural studies under pressure revealed a total and gradual conversion to the LS state in the interval of pressures comprised between 0.7-2.0 GPa.

The mononuclear compound [Fe(tpa)(NCS)$_2$] (tpa: tris(2-pyridylmethyl)amine)) exhibits one-step spin transition at atmospheric pressure. Single-crystal-to-single-crystal transformation occurs upon exposure of the complex to methanol vapours resulting in a new compound, {[Fe(tpa)(NCS)$_2$]·[Fe(tpa)(NCS)$_2$·CH$_3$OH]}. The new complex contains two distinct Fe(II) crystallographic sites one of which features strong hydrogen-bonding interactions with methanol molecules in the solid state. It shows a continuous two-step spin conversion and the [HS–LS] state has been crystallographically resolved: (Fe1(HS)-Fe2(LS)). Application of pressure minimizes the differences in the crystal field strength of the iron(II) sites. Indeed, the two-step transition transforms into a one-step with a considerable amount of Fe(II) molecules in the LS state at room temperature. At pressures as high as 1 GPa the complex is in the LS state. By contrast, the one-step spin transition of the pristine compound converts to a two-step transition under pressure. As pressure increases the characteristic temperatures are shifted to higher temperatures [168].

The complex [Fe(mtz)$_6$](BF$_4$)$_2$ (mtz = methyltetrazole) possesses two distinct Fe(II) crystallographic sites. The crystal field strength at one of the iron sites is stronger and undergoes one-step spin transition at low temperature (75 K).

Low pressures (0.14 GPa) shift the transition temperature up to 100 K, and the application of 0.57 GPa results in SCO being induced at the other Fe(II) site. At 0.81 GPa the spin transition is continuous, complete and is centred at around 180 K, as shown in Figure 12 [82]. Similar observations were reported also on the compound Fe(3-methylpyridine)$_2$[Ni(CN)$_4$] [169].
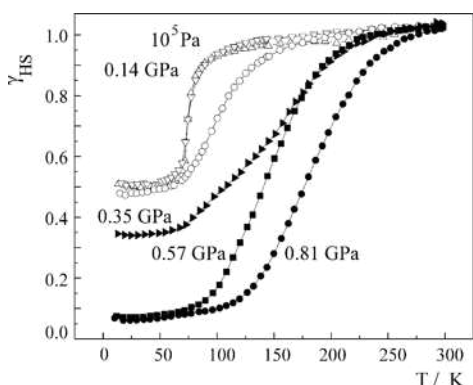

Figure 12. High spin fraction as a function of the temperature at distinct hydrostatic pressures for complex [Fe(mtz)$_6$](BF$_4$)$_2$. Reprinted from [82] **Copyright (2005), with permission from Elsevier**

An anion order-disorder transition has been proved to be the driving force for the two-step thermal spin transition in the mononuclear compound [Fe(L)$_2$](ClO$_4$)$_2$ (L = 2,6-bis{3-methylpyrazol-1-yl}-pyrazine). The first step of the spin transition curve is abrupt, concomitant with an isostructural phase transition provoked by the cessation of dynamic anion disorder on lowering the temperature. The second step is more continuous. High pressure single crystal X-ray diffraction and Raman spectroscopy studies performed up to 2 GPa have revealed a similar mechanism for the pressure-induced spin crossover [126].

The mononuclear compounds [Fe(bapbpy)(NCS)$_2$] (bapbpy = 6,6' -bis(amino-2- pyridyl)-2,2'-bipyridine) [79] and [Fe(5-NO$_2$-sal-N(1,4,7,10))] [82] exhibit a two-step spin transition accompanied with hysteresis at atmospheric pressure. Application of pressure discloses a very particular behaviour of the two-step transition curve: -parallel shift to higher temperature and increase of the hysteresis width as pressure increases, as shown in Figure 13. Detailed structural analysis in the case of [Fe(bapbpy)(NCS)$_2$] revealed that the same series of phase transitions occurs both on cooling and on application of pressure, and variable temperature and pressure XRD experiments allowed the structural phase diagram to be experimentally plotted for the first time [79].
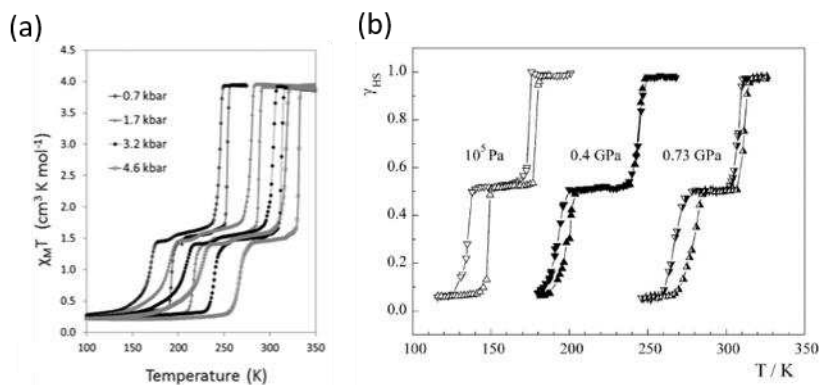
Figure 13. (a) Magnetic properties under hydrostatic pressure for [Fe(bapbpy)(NCS)₂] Reprinted with permission from [79] **Copyright (2011) by the American Physical Society (b) Magnetic properties under hydrostatic pressure for [Fe(5-NO₂-sal-N (1,4,7,10))]. Reprinted from** [82] **Copyright (2005), with permission from Elsevier**

The two-dimensional (2D) square-grid type porous coordination polymer [Fe(bdpt)₂]·guest (Hbdpt = 3-(5-bromo-2-pyridyl)-5-(4-pyridyl)-1,2,4-triazole, guest = EtOH and MeOH) shows a two-step spin transition accompanied by a re-entrant crystallographic phase transition [100% HS ($P2_1/n$) $\leftrightarrow$ [50% HS–50% LS] (P-1) $\leftrightarrow$ 100% LS ($P2_1/n$)]. In Figure 14 the magnetic properties at different hydrostatic pressures of the guest-free framework and those of the frameworks loaded with ethanol and methanol are shown [152]. At 10^{-4} GPa the highest transition temperature of the two-step process is observed for the guest-free framework and the lowest for the framework loaded with EtOH. Interestingly, for pressures below 0.5 GPa the second step of the spin transition is shifted to lower temperatures and the hysteresis width increases for all compounds. In contrast, the first step is shifted to higher temperatures and the displacement is approximately 70 K at 0.72 GPa for the MeOH loaded framework. The hysteresis width also increases for the first step, being 2 K for all compounds at the highest pressure applied (0.7-0.8 GPa). Both thermal and pressure induced SCO in the guest-loaded frameworks are influenced by the steric effects imposed by the guest molecules which provoke the stabilisation of the HS state and hence displacement of the T_c (second step) to lower temperatures. For the guest-free framework the stabilization of the intermediate state [50% HS–50% LS] (P-1) occurs on lowering the temperature or increasing the pressure.
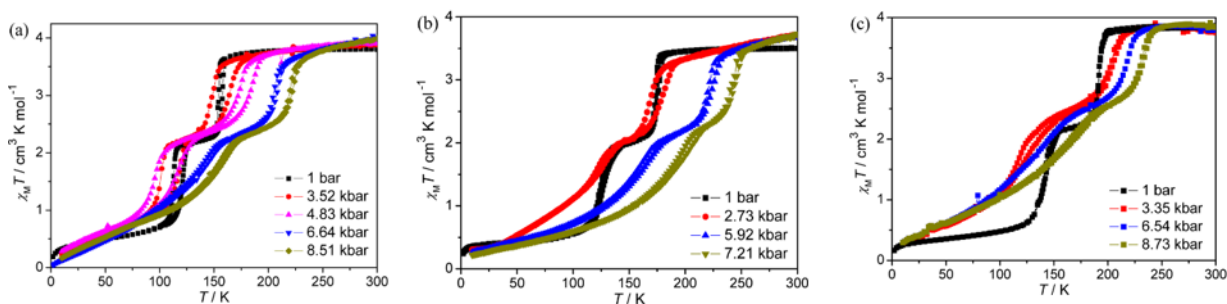
Figure 14. χMT vs T plots at different hydrostatic pressures for [Fe(bdpt)2]·G: a) G = EtOH, b) G = MeOH and c) guest-free framework. Reprinted with permission from [152]. **Copyright (2012) American Chemical Society.**

3.4. Paramagnetic compounds

The effect of hydrostatic pressure on the paramagnetic, ferromagnetic or antiferromagnetic behaviour of several Fe(II) coordination complexes have been studied. For example, a complete thermal spin transition in the interval of

pressures from 0.5 to 1 GPa have been reported for the mononuclear complexes [Fe(abpt)₂(NCS)₂] polymorph B [139] and [Fe(stpy)₄(NCBH₃)₂]cis [141], which are paramagnetic (i.e. not SCO-active) under atmospheric pressure (Figure 15). These studies corroborate the expected modification of the ligand field strength and the stabilisation of the LS state under the application of external hydrostatic pressure. The induced thermal spin transitions are continuous and the equilibrium temperatures are displaced to higher temperature as pressure increases. For compound [Fe(abpt)₂(NCS)₂] polymorph B, $T_{1/2}$ at the highest pressure investigated (1.05 GPa) is 179 K while it is 175 K for complex [Fe(stpy)₄(NCBH₃)₂]cis at 0.7 GPa. Both compounds show a linear dependence of $T_{1/2}$ with pressure.
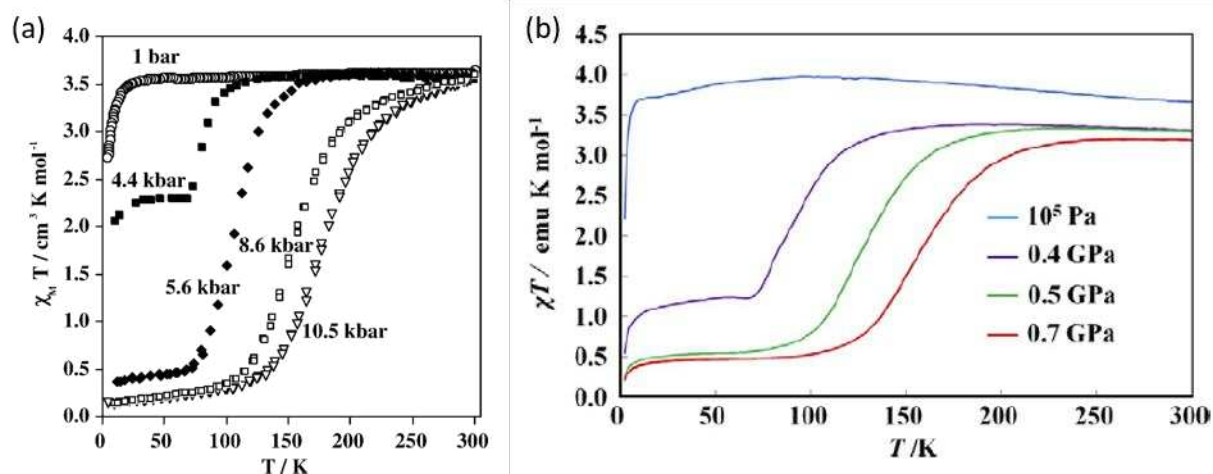

Figure 15. (a) Thermal variation of the molar magnetic susceptibility, $\chi_M T$, for [Fe(abpt)₂(NCS)₂] polymorph B at different hydrostatic pressures. Reprinted by permission from Springer Nature [139] (b) Thermal variation of the molar magnetic susceptibility, $\chi_M T$, for [Fe(stpy)₄(NCBH₃)₂]cis at different hydrostatic pressures. Reprinted from [141], Copyright (2011), with permission from Elsevier

Other remarkable studies of paramagnetic complexes under pressure concerns the dinuclear {[Fe(bpm)(NCS)₂]₂bpm} and the one-dimensional [Fe(bpm)(NCS)₂]ₙ compounds based on the 2,2'-bipyrimidine bridge ligand [73]. Coexistence of antiferromagnetically coupled [HS–HS] pairs and spin transition has been proved for the dinuclear complex under the application of pressure. At 0.63 GPa, nearly 50% of the [HS–HS] pairs transforms into the [HS–LS] pairs (Figure 16). Further increase of pressure until 0.89 GPa provokes the total conversion of the [HS–HS] pairs to the magnetically uncoupled [HS–LS] pairs. The magnetic behaviour of the one-dimensional [Fe(bpm)(NCS)₂]ₙ complex is very similar to that of the dinuclear ones with the difference that the spin transition, [···HS–HS···] ↔ [···LS–HS···], takes place at higher pressures (1.18 GPa).

 As far as the study of paramagnetic 2D polymers under pressure is concerned the porous Hoffman-like polymer [FePd(CN)₄(thiome)₂]·2H₂O [thiome = (4-[(E)-2-(5-methyl-2-thienyl)vinyl]-1,2,4-triazole] represents an interesting example [170]. Steric effects hinder the spin transition when water molecules are located within the layered structure. However, at 0.68 GPa, a two-step spin transition is observed in the interval of temperatures of 300-100 K (Figure 16). The first step is more abrupt and occurs within 30 K while the second one is more continuous but accompanied by hysteresis. This result suggests that the layers distort to accommodate the volume change of the structure on going from the HS to the LS state. Moreover, the application of pressure strengthens the intermolecular interactions leading to a cooperative spin transition as that observed for the guest-free compound [FePd(CN)₄(thiome)₂].

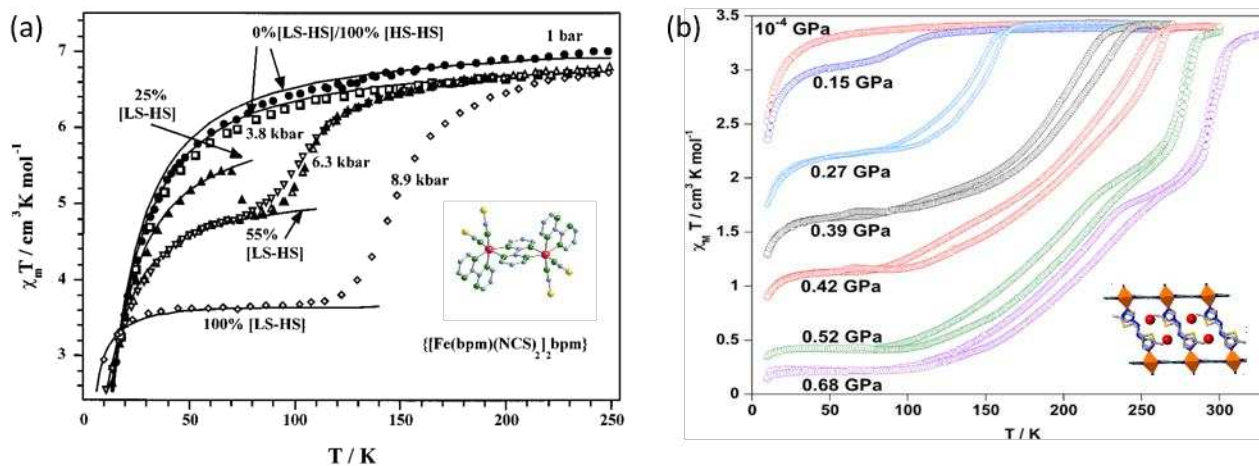**Figure 16. (a)** Temperature dependence of $\chi_m T$ for {[Fe(bpm)(NCS)$_2$]$_2$bpm} at different hydrostatic pressures. . Reprinted with permission from [73]. Copyright (2001) American Chemical Society. **(b)** Temperature dependence of $\chi_m T$ for [FePd(CN)$_4$(thiome)$_2$]·2H$_2$O at different hydrostatic pressures. Reprinted with permission from [170]. Copyright (2016) American Chemical Society.

The 3D cyanide-based framework {[Fe(pyrazole)$_4$]$_2$[Nb(CN)$_8$]·4H$_2$O}$_n$ presents a diamond-like structure with the iron and niobium ions connected through CN bridging ligands [104]. At ambient pressure, the compound exhibits a ferromagnetic behaviour with a Curie temperature of 9.4 K as a result of the antiferromagnetic coupling between neighbouring Fe(II) (HS, S = 2) and Nb(IV) (S = ½) metal centres. The magnetic behaviour of the complex changes dramatically due to the pressure-induced spin transition at the iron(II) centres, which is almost complete at 1.0 GPa (Figure 17). As pressure increases χT gradually decreases denoting the presence of a percentage of Fe(II) ions in the diamagnetic LS state. At 0.5 GPa the magnetic order switches from ferrimagnetic to antiferromagnetic. For pressures above 1.0 GPa, with all the Fe(II) centres in the LS state, the magnetic order disappears and the compound exhibits a paramagnetic behaviour arising from the niobium ions.
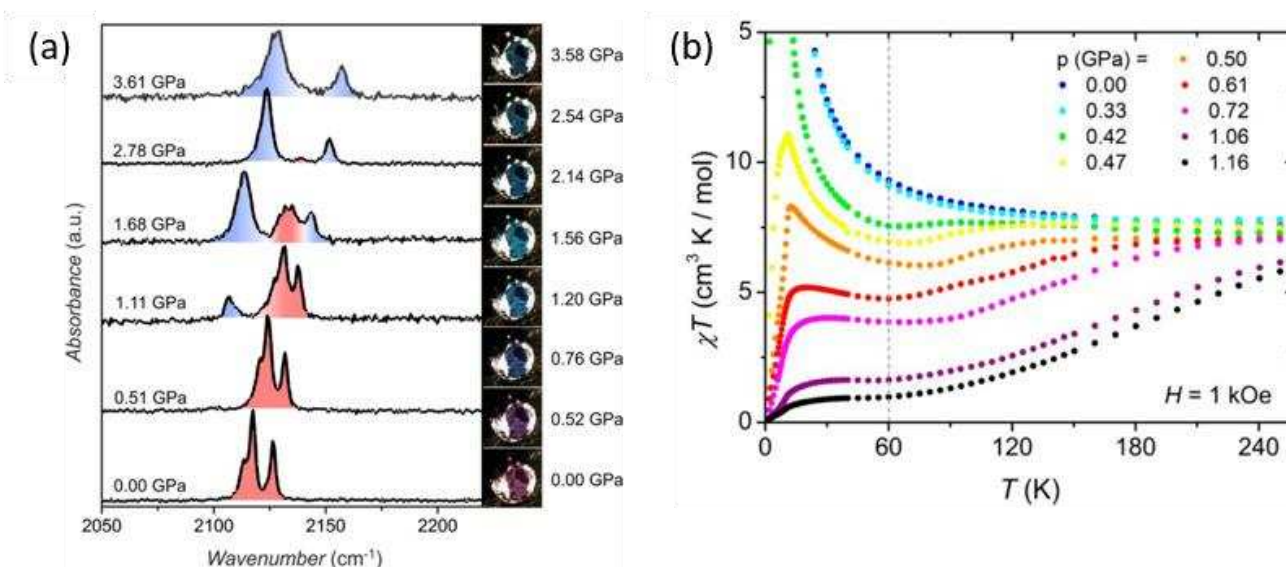
Figure 17. (a) Raman spectra of compound {[Fe(pyrazole)$_4$]$_2$[Nb(CN)$_8$]·4H$_2$O}$_n$ under pressure at room temperature. The photographs acquired at different pressures evidence the piezochromic effect of the compound (HS: pink-violet and LS: blue). **(b)** Magnetic properties in the form of $\chi_M T$ vs T at different pressures. Reprinted with permission from [104] https://pubs.acs.org/doi/abs/10.1021/jacs.5b04303.

4. Pressure effect studies on Cr(II), Mn(III) and Fe(III) coordination compounds

The number of complexes of reported Cr(II) and Mn(III) undergoing SCO is very small, while more examples have been reported for Co(II) and Fe(III) ions [171]. Below are described a few studies of the pressure effect on the spin transition properties of these metal complexes.

A thermal spin transition in a Cr(II) compound was firstly reported for [CrI$_2$(depe)$_2$] (depe: 1,2-bis(diethylphosphino)ethane) [172]. The sharp spin transition between the $^3T_{1g}$ (S = 1) and ^5E_g (S = 2) electronic states taking place at T$_{1/2}$ = 169 K at ambient pressure is displaced progressively to higher temperatures as pressure increases (Figure 18a) [137]. Under pressure the transition becomes more continuous and at 0.8 GPa the compound is in the LS state at room temperature. The dependence of $T_{1/2}$ with pressure is linear for pressures above 0.3 GPa when the Cr-P bond lengths are noticeably altered by pressure. At relatively low pressures the large iodine ions compress and the Cr-P distances remain unaltered.

The compound [Fe(sal$_2$-trien)][Ni(dmit)$_2$] exhibits one of the most cooperative spin transitions reported for an Fe(III) SCO compound. It undergoes a spin transition between the S = 5/2 and S = 1/2 spin states around 245 K accompanied by a large hysteresis loop of 30 K. Pressure effect studies reveal that at pressures as low as 0.05GPa the hysteresis loop becomes wider (60 K) and only half of the Fe(III) centres switch to the LS state [173]. Further increase of pressure up to 0.7 GPa displace the transition temperature upwards but the hysteresis width and the percentage of Fe(III) molecules in the LS state remain unaltered. After realising the pressure the spin transition observed at 10^{-4} GPa is not recovered suggesting that the compound experienced and irreversible structural phase transition under pressure.

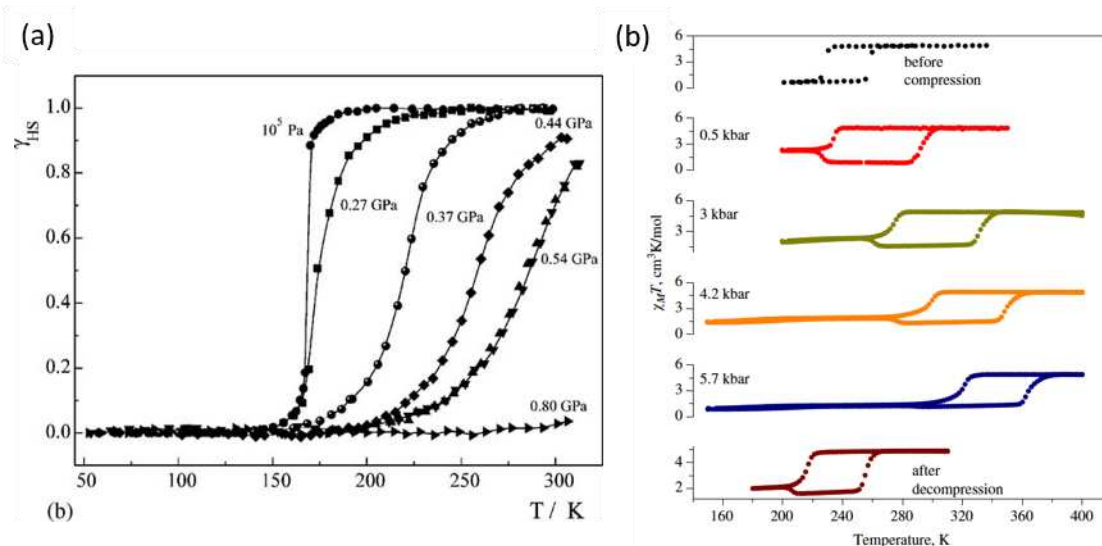
Figure 18. (a) High spin fraction *vs* temperature, γ_{HS} *vs* T, for compound [CrI$_2$(depe)$_2$] at different hydrostatic pressures. Reprinted with permission from [137]. Copyright (2004) American Chemical Society. (b) Temperature dependence of χ_MT for [Fe(sal$_2$-trien)][Ni(dmit)$_2$] at different pressures. Reprinted from [173] Copyright (2008), with permission from Elsevier.
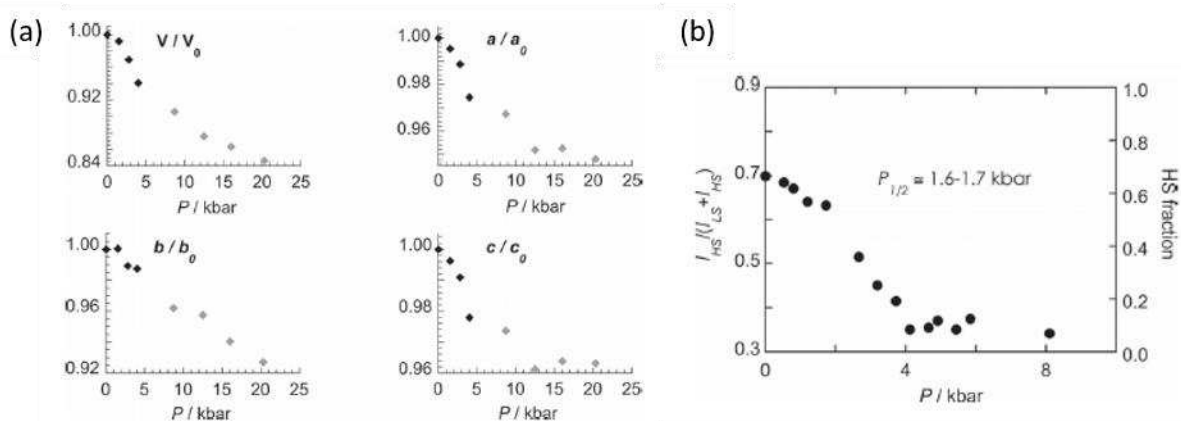
Figure 19. a) Pressure dependence of the unit cell parameters of a single crystal of [(TPA)Fe(TCC)](SbF$_6$) at 293 K. (b) HS fraction as a function of applied pressures at 293 K for complex [(TPA)Fe(TCC)](SbF$_6$) derived from the Raman spectra. Reproduced from [174] with permission.

The [(TPA)Fe(TCC)](SbF$_6$) complex [TPA = tris(2-pyridylmethyl)amine and TCC^{2-} = 3,4,5,6-tetrachlorocatecholate dianion] exhibits an incomplete $S = 1/2 \leftrightarrow S = 5/2$ thermal spin-crossover process centred at 250 K at ambient pressure [174]. By contrast, a complete transition to the $S = \frac{1}{2}$ state is induced at relatively small pressures (0.45 GPa) at room temperature as Raman experiments demonstrate (Figure 19). The spin state conversion is gradual with $P_{1/2} = 0.16$-0.17 GPa. The crystal structure of the complex has been studied under pressure as well. In Figure 19a are depicted the evolution of the unit cell parameters as a function of pressure. Below 0.4 GPa the decrease in the volume of the unit cell (ca. 8%) as well as in the a, b and c parameters as pressure increases denotes the expected contraction of the crystal lattice as a result of the spin crossover process. For higher pressures the compression of the LS unit cell volume becomes smoother. The compression of the cell is markedly pronounced in the ac plane where the complex cations [(TPA)Fe(TCC)]$^+$ are located. Indeed, pressure enhances the hydrogen bonding interactions between the complex cations. The cations and anions stack along the b direction and its mutual compression results in a contraction of the b axis (15% at 2 GPa).

The porphyrin Fe(III) complex [Fe(PPIX)OH] has been investigated under pressure using Mössbauer spectroscopy [175]. Like observed for other porphyrin compounds a $S = 5/2$ high spin to $S = 5/2$, $3/2$ admixed spin state transition of the Fe(III) site takes place at pressures above 2.2 GPa. Pressure induces the ligand movement towards the iron centre and movement of the Fe ion towards the porphyrin plane, which leads to the electronic transition.

The [Mn(pyrol)$_3$tren] complex exhibits a very abrupt spin transition from the HS (^{5}E) to LS state (^{3}T$_1$) at low temperature (44 K). The crystal structure studies performed at room temperature evidenced that the complex remains the HS state at 1.00 GPa. The crystal structure of the HS state under pressure is very similar to that of the complex in the LS state. The differences are the metal-to-ligand bond distances and the intermolecular contacts, which are slightly shorter under pressure. These studies clearly demonstrated that the spin transition in the complex is not connected to the internal pressure in the crystal. Most likely the spin transition is connected to the dynamic Jahn-Teller effect on the Mn(III) ion [78].

5. Theoretical Aspects

In order to better understand the pressure influence on spin crossover complexes several types of models has been proposed, including: thermodynamic [6,27,136,176], Ising-like [111,165,177,178], or mechano-elastic models [179–183]. Since the Ising-like and mechano-elastic models are described in more detail in other papers of this special issue, herein we will only discuss the thermodynamic approach. It should be noted that thermodynamic and Ising-like models are completely equivalent in the mean-field approach [184].

The first model that describes the pressure effect on molecular spin crossover complexes was proposed in 1972 by Slichter and Drickamer [6], starting from thermodynamic considerations. This model represented the starting point for many macroscopic models attempting to describe the origin of the interactions (atom-phonon coupling, elastic energy, etc.). It is based on the theory of regular solutions assuming a mixture of both HS and LS species with their Gibbs free energy G_{HS} and G_{LS}, respectively. Thus, the free energy for the mixture of the interacting centers is expressed as:

$$G = n_{LS}G_{LS} + n_{HS}G_{HS} - TS_{mix} + \Gamma n_{HS}n_{LS} \tag{6}$$

Where n_{LS} and n_{HS} are the associated mole fractions of the LS and HS states, respectively; Γ is a phenomenological intermolecular interaction parameter which indicates that the free energy may depend on the site fraction, and S_{mix} is the entropy of mixing for and ideal solution of LS and HS molecules, given by $S_{mix} = -R(n_{LS} \ln n_{LS} + n_{HS} \ln n_{HS})$ with R being the gas constant. If G_{LS} is considered as the origin level for energies then $G_{LS} = 0$ while $G_{HS} = \Delta G = \Delta H - T\Delta S$, with ΔH and ΔS are the entropy and the enthalpy variations, respectively, during the spin transition. As a consequence, the free energy can be written as follows:

$$G = n_{HS}\Delta H + \Gamma n_{HS}\left(1 - n_{HS}\right) - RT\left[\left(1 - n_{HS}\right)\ln\left(1 - n_{HS}\right) + n_{HS}\ln n_{HS} + n_{HS}\frac{\Delta S}{R}\right] \tag{7}$$

The equilibrium condition of the system, $\left(\frac{\partial G}{\partial n_{HS}}\right)_{T,p} = 0$, leads to the implicit expression of n_{HS} as a function of temperature, T:

$$T = \frac{\Delta H - \Gamma\left(1 - 2n_{HS}\right)}{R\ln\left(\dfrac{1 - n_{HS}}{n_{HS}}\right) + \Delta S} \tag{8}$$

An illustration of the effect of the intermolecular interaction constant on the thermal variation of n_{HS} is shown in Figure 20.
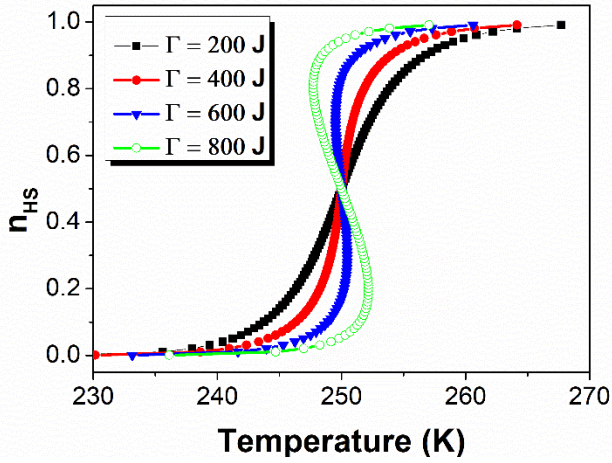
Figure 20. Thermal variations of the HS molar fraction for four selected values of the intermolecular interaction constant Γ = 200 J, 400 J, 600 J and 800 J. The following values have been used for the enthalpy and entropy variations: ΔH = 15 kJmol^{-1}, ΔS = 70 kJmol^{-1}.

The pressure effect has been taken into account expressing the variation of the free energy as:

$$\Delta G = \Delta G(0) + p\Delta V + \frac{p^2}{2}\Delta\frac{V(0)}{B} \qquad (9)$$

where B is the bulk modulus at ambient pressure.

The first term represents the contribution from the free energy difference at zero pressure, the second term is due to the fact that the two species have different volumes, and the third term corresponds to the fact that the two species have different bulk moduli.

The effect of pressure on the temperature induced spin transition as well as the temperature on the pressure induced spin transition calculated in the framework of Slichter and Drickamer model are reported in Figure 21.
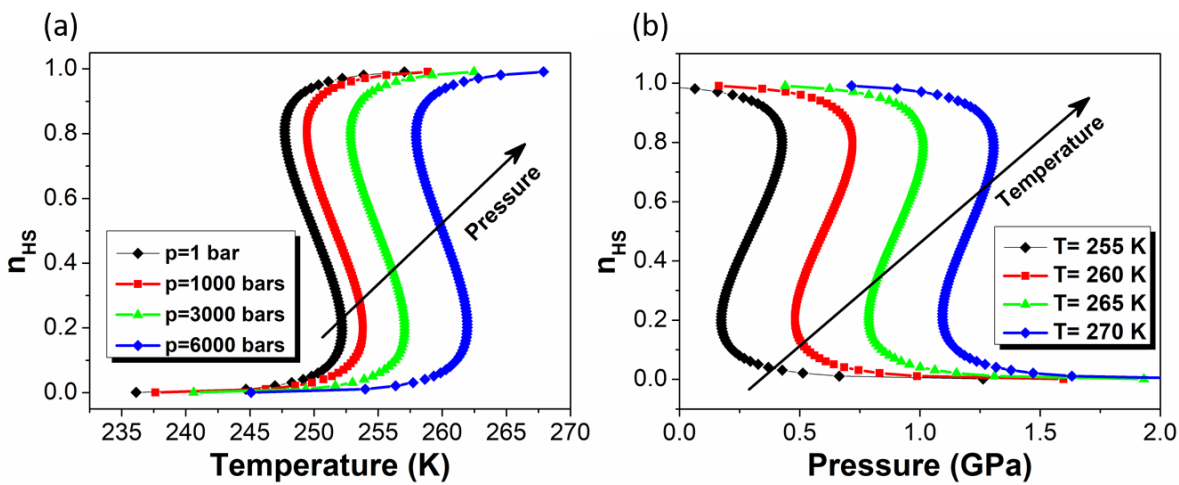

Figure 21. (a) Thermal variations of the HS molar fraction for various external pressures and (b) The Pressure induced spin transition, simulated for various temperature values. The following values have been used for the enthalpy and entropy variations: ΔH = 15 kJmol^{-1}, ΔS = 70 kJmol^{-1}, ΔV = 10 Å^3.

Thus, the model proposed by Slichter and Drickamer can successfully describe the typical behaviour of the spin crossover complexes, i.e. the shift of the characteristic transition temperatures towards higher temperatures, as shown in Figure 20, and a decrease of the hysteresis width with increasing pressure, as shown in Figure 21. However, it cannot explain some of the more unusual behavior (discussed in Section 3) such as increasing width of hysteresis. In this context, Ksenofontov and collaborators have extended the mean field approximation approach to indirect couplings of pressure to the order parameter by taking into account the pressure dependence of the bulk modulus of the complex within elasticity theory [50]. By taking into account the lattice elastic energy the Gibbs free energy can be written as:

$$G(p,T) = (\Delta F_{HL} + \Delta_{el} + p\Delta V)n_{HS} - TS_{mix} - \Gamma n_{HS}^2 \qquad (10)$$

Where ΔF_{HL} is the electronic contribution and Δ_{el} is the elastic energy, given by the following relation:

$$\Delta_{el} = \frac{1}{2}B\frac{\gamma_0 - 1}{\gamma_0}\frac{\Delta V}{V_0}(V_{HS} + V_{LS} - 2V_0). \qquad (11)$$

γ_0 is the Eschelby constant wich relates the local volume changes V_{HS}-V_{LS} of the molecule to the volume change of the lattice $\Delta V = \gamma_0(V_{HS} - V_{LS})$. V_0 is the volume provided by the lattice for the molecule. The mean value $\frac{1}{2}(V_{HS} + V_{LS})$ as compared to the volume V_0 indicates the sign of the elastic energy.

Spiering et al. set up the complete free energy of the whole system, such that the HS fraction as well as the volume and anisotropic deformations are freely varying parameters [136,176]. In the model proposed by Spiering et al. the spin transition centers are modelled as point defects and the crystal as an elastic, isotropic and homogenous medium, of spherical shape with only two elastic constants, the bulk modulus B and the Poisson ratio $0 \leq \sigma \leq 1/2$.

The elastic energy, (e_α) of the sphere, which has the volume v_α (α=HS, LS), placed in an elastic medium that provides a volume v_0 for its molecules can be written as follows:

$$e_\alpha = \frac{1}{2}B(\gamma_0 - 1)\left[\frac{(v_\alpha - v_0)^2}{v_0} - \gamma_0\frac{(v_\alpha - v_0)^2}{V}\right] \qquad (12)$$

where: γ_0 is the Eshelby constant and V is the volume of the crystal.

The first term represents the energy that appears due to the difference in volume of the crystal and the second term is correcting the surface effect of the crystal.

Thus, the total elastic energy for N sites, randomly distributed in an isotropic homogeneous elastic medium is given by the relation:

$$E = \frac{1}{2}B(\gamma_0 - 1)\sum\frac{(v_i - v_0)^2}{v_0} - \frac{1}{2}B\gamma_0(\gamma_0 - 1)\frac{[\sum(v_i - v_0)]^2}{V} \qquad (13)$$

The phonon free energy is approximated by the Debye model with a Debye temperature Θ dependent on volume by the Grüneisen approximation:

$$\frac{d\Theta}{\Theta} = -\gamma_G \frac{dV}{V} \Rightarrow \Theta(V) = \Theta_0 \left(\frac{V_0}{V}\right)^{\gamma_G} \tag{14}$$

Where the volume V_0 is the volume per molecule at zero K and γ_G is the Grüneisen constant.

The Grüneisen constant describes the change of the Debye frequency due to the anharmonicity of the lattice, as illustrated in Figure 22 [136].
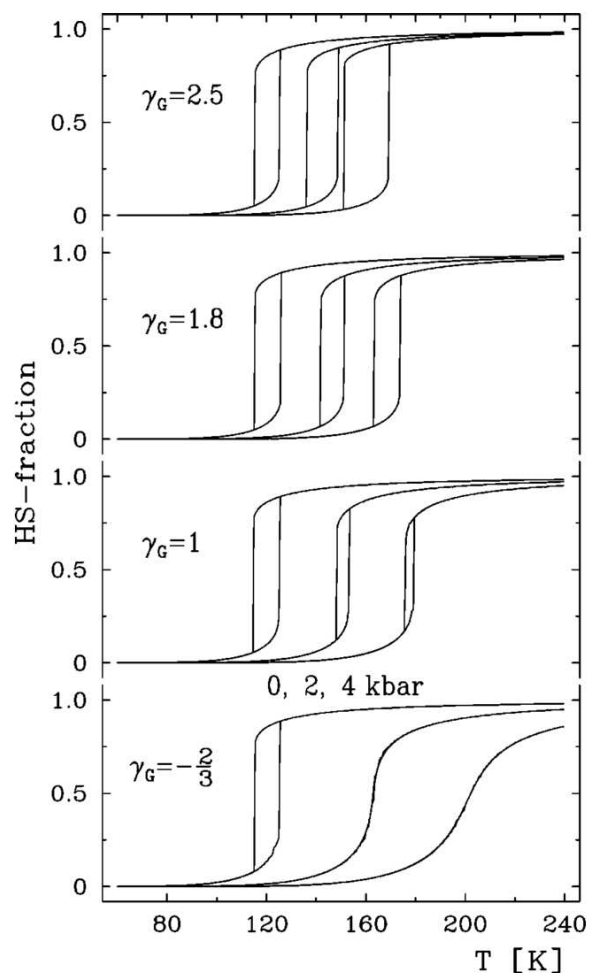

Figure 22. The effect of lattice anharmonicity simulated for a SCO system with a 10 K hysteresis width under an applied pressure up to 4 kbar. With increasing anharmonicity (γ_G from harmonic (−2/3) to 2.5) pressure favors hysteresis. At γ_G = 1.8 the width of the hysteresis is almost independent of pressure. At higher anharmonicity, γ_G = 2.5, an increasing of the hysteresis width with increasing pressure is observed. Reproduced from [136] with permission. Copyright 2004 by the American Physical Society.

A new approach was proposed by Levchenko et al. who used a microscopic model to analyse the behavior under pressure of molecular spin crossover complexes [148] by taking into account the contribution of phonons to the changes in spin state. In the framework of this model, the authors have shown that different experimental behavior of temperature- and pressure-induced spin transitions are determined by different variations of the inelastic and elastic energies under pressure, and the vibrational component of the free energy drives the spin transition equally with the electronic part. In other words, the (p,T) phase diagram will depend on the nature of the external stimuli. The model takes into account the pressure and temperature influence on the spin state, considering a symmetric deformation of the complexes and of the elastic medium.

The pressure effect on the spin state switching has been also investigated by First-Order Reversal Curve (FORC) diagram method. The FORC diagram method provides detailed information from within the major hysteresis loop, which enables determination of the distribution of switching temperatures and interaction fields for all of the "particles" that contribute to the hysteresis loop [185]. The measurement of a FORC begins with the saturation of the sample in HS (LS) state. The temperature is then ramped down (up) to a reversal temperature T_a. The FORC consists of a measurement of the high spin fraction as the temperature is then increased from T_a back up (down) to saturation. The high spin fraction at T_b on the FORC with reversal point T_a is denoted by $n_{HS}(T_a, T_b)$ (see Figure 23).
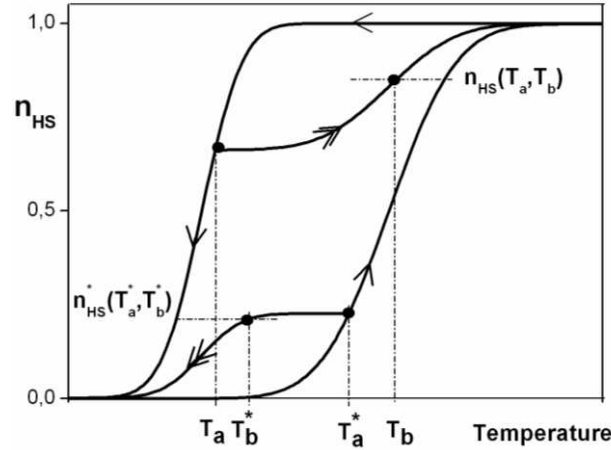

Figure 23. Definition of a thermal FORC in warming/cooling mode.

The temperatures steps are chosen such that T_a and T_b are regularly spaced, which means that $n_{HS}(T_a, T_b)$ can be plotted on a regular grid. The FORC distribution $\rho(T_a, T_b)$ is defined as the mixed second derivative

$$\rho(T_a, T_b) = -\frac{\partial^2 n_{HS}(T_a, T_b)}{\partial T_a \partial T_b}$$ and plotted in rotated coordinates from switching temperature $\{T_a, T_b\}$ to bias-coercivity $\{b = \frac{T_a + T_b}{2}, c = \frac{T_a - T_b}{2}\}$.

The FORC distribution is determined at each point by fitting a mixed second-order polynomial of the form $a_1 + a_2 T_a + a_3 T_b + a_4 T_a^2 + a_5 T_b^2 + a_6 T_a T_b$ to a local moving grid. In this case the value of $-a_6$ provides the mixed second derivative of the fitted surface and it can be assigned to the centre of grid as a representation of the density of the FORC distribution $\rho(T_a, T_b)$ at that point. The FORC diagrams can be interpreted in terms of distributions of the physical parameters: energy gap, Δ and interaction parameter, J.

Rotaru et al. have been analysed the thermal behaviour of the spin transition complexes [Fe$_x$Zn$_{1-x}$(btr)$_2$(NCS)$_2$]H$_2$O (for x=0.6 and x=1) by diffuse reflectivity measurements, under constant pressure in the range 1-1600 bars obtained with a gas pressure cell [186]. In their study an increase of both Δ and J with increasing pressure has been observed, as shown in Figure 24.
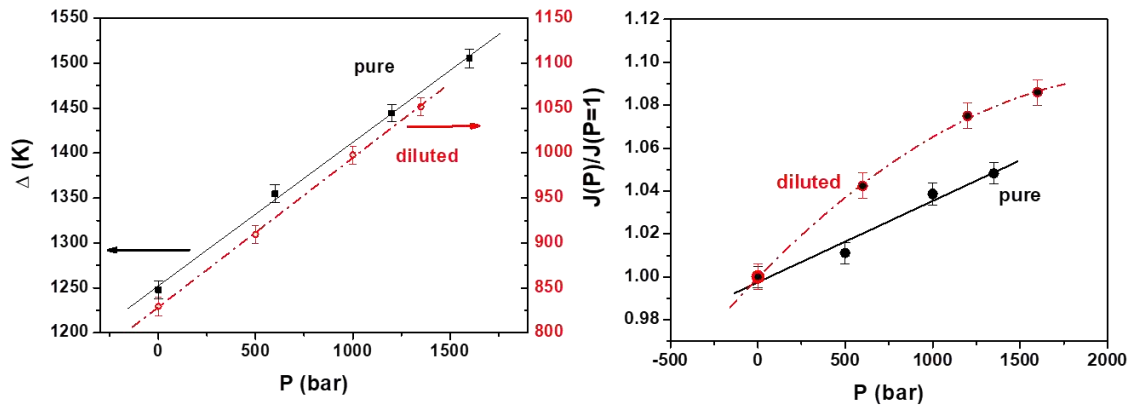
Figure 24. The pressure dependence of the average values of electronic gap (left) and interaction parameter J (right). Reprinted with permission from [186] **Copyright 2011 by the American Physical Society**

It was also shown that, for the pure compound, the J-Δ distributions remain uncorrelated in the whole pressure range which confirms that these distributions originate from independent mechanisms. An unexpected feature concerning the correlation parameter in the diluted compound, that is, a large decrease induced by pressure has been observed, as shown in Figure 25. In terms of composition distributions it means that, the like-spin domain size is increased by the applied pressure. These data have been interpreted by assuming that the pure compound has single-domain behaviour and the diluted one, multiple-domain behaviour, in agreement with the expectations derived from the optical microscopy.
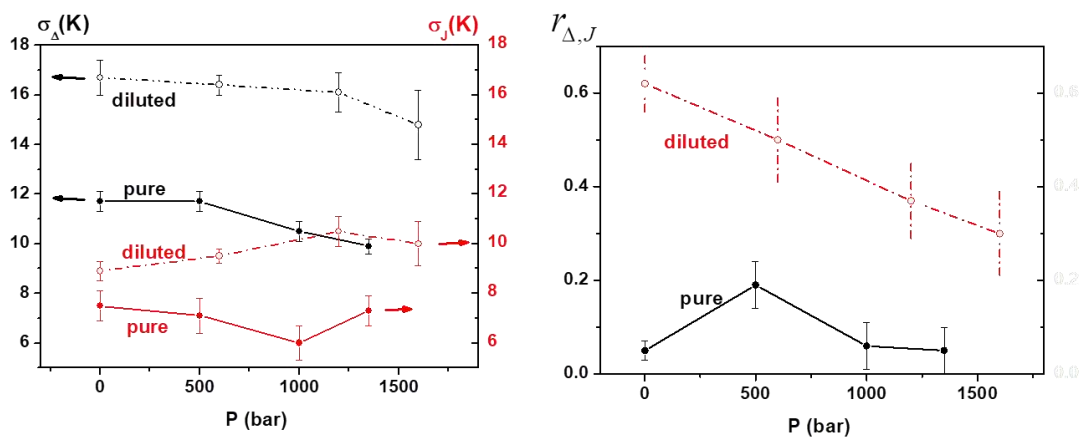
Figure 25. The pressure effect on the standard deviations and correlation parameters. Reprinted with permission from [186] **Copyright 2011 by the American Physical Society**

6. Summary and Perspectives

We have described the major techniques so far used to probe the spin crossover phenomenon at high pressure. Our aim was to shed some light on equipment, experiments, materials and theoretical approaches for high pressure research that together advance our fundamental understanding of SCO. We hope that by charting how high pressure SCO research has developed since its earliest days we can provide newcomers to the field with the tools required to push the boundaries yet further. Here we summarise what we believe to be some of the most important and promising areas for the future development of high pressure SCO research.

We have shown how important high pressure structural studies can be in rationalising unusual SCO behaviour on a case by case basis, and highlighted the importance of multiple complimentary techniques to rationalise behaviour. However, examples of such studies using multiple techniques are still exceptionally scarce. More studies on a wide range of samples, each in the exact same environment are required to unambiguously assess more general correlations between the structure of a material and its SCO properties. As the number of such studies increases it is important that their reliability and repeatability are ensured through careful attention to hydrostatic conditions within the pressure cell. Occasionally somewhat ignored in experimental sections in the literature, the pressure transmitting medium and method of applying pressure must be carefully considered in advance of the experiment and fully reported.

Despite the importance of hydrostatic conditions to high pressure experiments it is also interesting to consider the possibility of deliberate application of non-hydrostatic forces to SCO materials. To the best of our knowledge, no systematic studies aiming to quantify the effect of non-hydrostatic conditions on oriented spin crossover materials have yet been published. However in real-world applications, SCO materials are more likely to encounter non-hydrostatic stress during manufacturing and use. Such investigations could also reveal important insights on the role of anisotropy, which is often encountered in the structure and mechanical properties of ordered SCO solids [187]. Experimental methods for achieving this must be able to clearly control and quantify the direction and magnitude of the applied anisotropic force. Thus AFM studies of localised pressure on well oriented samples may well allow such detailed analysis, and we look forward to results in this area.

The importance of elastic interactions for SCO processes is clear, and yet very few experimental determinations of the elastic properties of SCO materials exist to date. High pressure studies present interesting opportunities to investigate lattice dynamics (compressibility, anharmonicity etc. and structure under pressure to rationalise cooperativity [136] and to evaluate potential applications in mechanical actuators [188]. The extension of this approach towards SCO nanomaterials, which are of vivid interest currently [189], may also allow to probe interactions between nano-objects as well as with their environment (matrix effects).

Under pressure, the dynamic and mechanical properties of the lattice that influence the phase transition are significantly altered from ambient conditions and thus domain formation and propagation events must also be very different. High pressure thus allows for the fine-tuning of inter- and intra-molecular interactions, permitting systematic investigation of their effect on the elastic stiffness of the lattice and hence on the observed switching behaviour. Spatio-temporal studies of SCO materials under pressure could prove fascinating, allowing the development of more advanced theoretical approaches and possibly even the design of novel materials with improved cooperativity. Time-resolved studies of SCO materials at ambient pressure are described in detail elsewhere in this issue. Performing time-resolved photo-induced switching experiments at high pressure rather than low temperature would allow the investigation of the effect of elastic properties on these dynamic processes, something that has remained conspicuously uncharted for phase transition materials at short time-scales. We highlighted the importance and complexities associated with obtaining hydrostatic conditions even in isothermal high pressure experiments. The difficulties are compounded as temperature varies, and have the potential to vary significantly during laser pulses. Quantifying the effect of these stimuli on the hydrostaticity of the sample environment may well present experimental

challenges, but would again be of fundamental importance to the interpretation of results in this area.

All of these experimental developments promise to supply increasingly reliable and numerous high pressure investigations of spin crossover materials that can both inspire and respond to the development of improved theoretical models. In particular, we anticipate that with increasing access to high pressure structures, *ab-initio* and molecular dynamics calculations will gain in importance in rationalizing the behaviour of SCO materials under pressure.

Conflicts of Interest

The authors declare no conflicts of interest.

References

[1]   P. Guionneau, Crystallography and spin-crossover. A view of breathing materials, Dalt. Trans. 43 (2014) 382–393. doi:10.1039/C3DT52520A.

[2]   H.G. Drickamer, Pressure tuning of electronic energy levels, Int. Rev. Phys. Chem. 2 (1982) 171–196. doi:10.1080/01442358209353334.

[3]   J.R. Ferraro, L.J. Basile, L. Sacconi, High spin-low spin crossover in Co(II) complexes with tris(2-diphenylphosphinoethyl)amine (NP$_3$) by application of high external pressures, Inorganica Chim. Acta. 35 (1979) L317–L318. doi:10.1016/S0020-1693(00)93380-2.

[4]   J.R. Ferraro, K. Nakamoto, J.T. Wang, L. Lauer, Conversion of distorted tetrahedral bis(benzyldiphenylphosphine)dibromonickel(II) into a pure planar complex by high pressure, J. Chem. Soc. Chem. Commun. (1973) 266. doi:10.1039/c39730000266.

[5]   H.G. Drickamer, C.W. Frank, Spin Changes in Iron Complexes, in: Electron. Transitions High Press. Chem. Phys. Solids, Springer Netherlands, Dordrecht, 1973: pp. 126–151. doi:10.1007/978-94-011-6896-0_8.

[6]   C.P. Slichter, H.G. Drickamer, Pressure-Induced Electronic Changes in Compounds of Iron, J. Chem. Phys. 56 (1972) 2142–2160. doi:10.1063/1.1677511.

[7]   D.C. Fisher, H.G. Drickamer, Effect of Pressure on the Spin State of Iron in Ferrous Phenanthroline Compounds, J. Chem. Phys. 54 (1971) 4825–4837. doi:10.1063/1.1674758.

[8]   C.B. Bargeron, H.G. Drickamer, Effect of Pressure on the Electronic Structure of Complexes of Ferrous Iron with Substituted Phenanthrolines, J. Chem. Phys. 55 (1971) 3471–3482. doi:10.1063/1.1676601.

[9]   S.C. Fung, H.G. Drickamer, Effect of pressure on the carbon-iron bond in ferrocyanides and ferricyanides, J. Chem. Phys. 51 (1969) 4353–4359. doi:10.1063/1.1671801.

[10]   A.H. Ewald, R.L. Martin, E. Sinn, A.H. White, Electronic equilibrium between the $^6A_1$ and $^2T_2$ states in iron(III) dithio chelates, Inorg. Chem. 8 (1969) 1837–1846. doi:10.1021/ic50079a006.

[11] H.G. Drickamer, The Effect of High Pressure on the Electronic Structure of Solids, Solid State Phys. 17 (1965) 1–133. doi:10.1016/S0081-1947(08)60410-5.

[12] A.H. Ewald, R.L. Martin, I.G. Ross, A.H. White, Anomalous Behaviour at the $^6A_1$ - $^2T_2$ Crossover in Iron (III) Complexes, Proc. R. Soc. A Math. Phys. Eng. Sci. 280 (1964) 235–257. doi:10.1098/rspa.1964.0143.

[13] K.J. Haller, P.L. Johnson, R.D. Feltham, J.H. Enemark, J.R. Ferraro, L.J. Basile, Effects of temperature and pressure on the molecular and electronic structure of N,N′-ethylenebis(salicylideneiminato)nitrosyliron, Fe(NO)(salen), Inorganica Chim. Acta. 33 (1979) 119–130. doi:10.1016/S0020-1693(00)89464-5.

[14] J. R. Ferraro, Vibrational studies of solid inorganic and coordination complexes at high pressures, Coord. Chem. Rev. 29 (1979) 1–66. doi:10.1016/S0010-8545(00)80362-8.

[15] R.J. Butcher, J.R. Ferraro, E. Sinn, The nature of the high spin-low spin crossover in tris(N-ethyl-N-phenyldithiocarbamato)iron(III), Inorg. Chem. 15 (1976) 2077–2079. doi:10.1021/ic50163a012.

[16] R.J. Butcher, J. R.Ferraro, E. Sinn, Nature and Mechanism of high spin-low spin Crossovers and the existence of intermediate spin states, Chem. Commun. (Camb). 0 (1976) 910–912. doi:10.1039/C39760000910.

[17] J.R. Ferraro, L.J. Basile, L.R. Garcia-Ineguez, P. Paoletti, L. Fabbrizzi, Concerning the thermochromic mechanism of copper(II) and nickel(II) complexes of N,N-diethylethylenediamine, Inorg. Chem. 15 (1976) 2342–2345. doi:10.1021/ic50164a004.

[18] H.G. Drickamer, Electronic Transitions in Transition Metal Compounds at High Pressure, Angew. Chemie Int. Ed. English. 13 (1974) 39–47. doi:10.1002/anie.197400391.

[19] L. Sacconi, J.R. Ferraro, Pressure-temperature relationships of the spin-state equilibrium in a five-coordinate complex of cobalt(II) thiocyanate with an nnp tridentate ligand, Inorganica Chim. Acta. 9 (1974) 49–50. doi:10.1016/S0020-1693(00)89881-3.

[20] J.R. Ferraro, J. Takemoto, Pressure-Temperature Relationships for Fe(II) Complexes of 1,10-Phenanthroline and 2,2′-Bipyridine, Appl. Spectrosc. 28 (1974) 66–68. doi:10.1366/000370274774332957.

[21] E. Konig, Nature and Dynamics of the Spin-State Interconversion in Metal-Complexes, Struct. Bond. 76 (1991) 51–152. doi:10.1007/3-540-53499-7_2.

[22] C.P. Köhler, R. Jakobi, E. Meissner, L. Wiehl, H. Spiering, P. Gütlich, Nature of the phase transition in spin crossover compounds, J. Phys. Chem. Solids. 51 (1990) 239–247. doi:10.1016/0022-3697(90)90052-H.

[23] G.J. Long, B.B. Hutchinson, Spin Equilibrium in Iron(II) Poly(1-pyrazolyl)borate Complexes: Low-Temperature and High-Pressure Mössbauer Spectral Studies, Inorg. Chem. 26 (1987) 608–613. doi:10.1021/ic00251a023.

[24] P. Adler, L. Wiehl, E. Meibner, C.P. Köhler, H. Spiering, P. Gütlich, The influence of the lattice on the spin transition in solids. Investigations of the high spin ag low spin transition in mixed crystals of [Fe_xM_{1-x}(2-pic)$_3$]Cl$_2$·MeOH, J. Phys. Chem. Solids. 48 (1987) 517–525. doi:10.1016/0022-3697(87)90046-1.

[25] E. Meissner, H. Köppen, C.P. Köhler, H. Spiering, P. Gütlich, Anomalous pressure dependence of the Lamb-

Mössbauerf-factor in a spin crossover system [Fe(2-pic-ND$_2$)$_3$]Cl$_2$·EtOD, Hyperfine Interact. 36 (1987) 1–12. doi:10.1007/BF02396844.

[26]   S. Usha, R. Srinivasan, C.N.R. Rao, High-pressure magnetic susceptibility studies of spin-state transition in Fe(II) complexes, Chem. Phys. 100 (1985) 447–455. doi:10.1016/0301-0104(85)87069-5.

[27]   E. König, G. Ritter, J. Waigel, H.A. Goodwin, The effect of pressure on the thermal hysteresis of the first-order spin transition in bis(1,10-phenanthroline-2-carbaldehyde phenylhydrazone) iron (II) complexes, J. Chem. Phys. 83 (1985) 3055–3061. doi:10.1063/1.449209.

[28]   J. DiBenedetto, V. Arkle, H.A. Goodwin, P.C. Ford, Activation volumes for the quintet/singlet relaxation kinetics of iron(II) complexes, Inorg. Chem. 24 (1985) 455–456. doi:10.1021/ic00198a003.

[29]   E. Koenig, G. Ritter, S.K. Kulshreshtha, J. Waigel, H.A. Goodwin, The discontinuous high-spin (^{5}T$_2$) - low-spin (^{1}A$_1$)   transition   in   solid   bis(1,10-phenanthroline-2-carbaldehyde   phenylhydrazone)iron(II) bis(tetrafluoroborate): hysteresis effects, concurrent crystallographic phas, Inorg. Chem. 23 (1984) 1896–1902. doi:10.1021/ic00181a022.

[30]   Jü. Pebler, Reinvestigation of the Iron-57 Mössbauer Effect at High Pressures in Some Iron(II) Bis(phenanthroline) Complexes, Inorg. Chem. 22 (1983) 4125–4128. doi:10.1021/ic00168a059.

[31]   E. Meissner, H. Köppen, H. Spiering, P. Gütlich, The effect of low pressure on a high-spin-low-spin transition, Chem. Phys. Lett. 95 (1983) 163–166. doi:10.1016/0009-2614(83)85088-X.

[32]   D.M. Adams, G.J. Long, A.D. Williams, Spectroscopy at Very High Pressures. 36. An Infrared Study of Spin-State Equilibria in Some Iron(II) Complexes, Inorg. Chem. 21 (1982) 1049–1053. doi:10.1021/ic00133a036.

[33]   J.J. McGarvey, I. Lawthers, K. Heremans, H. Toftlund, Kinetics of Spin-State Interconversion in Iron(II) Complexes in Solution as a Function of Pressure: Activation Volumes for the ^{1}A$_1$ ⇌ ^{5}T$_2$ Spin Change, Inorg. Chem. 29 (1990) 252–256. doi:10.1021/ic00327a020.

[34]   G.J. Long, L.W. Becker, B.B. Hutchinson, A High-Pressure Mössbauer Effect Study of the Spin State in Bis[hydrotris(3,5-dimethyl-1-pyrazolyl)borate]iron(II),   in: 1981:   pp.   453–462.   doi:10.1021/ba-1981-0194.ch020.

[35]   J.K. McCusker, M. Zvagulis, H.G. Drickamer, D.N. Hendrickson, Pressure-induced spin-state phase transitions in dichloro- and dibromobis[cis-1,2-bis{(diphenylphosphino)ethylene}]iron, Inorg. Chem. 28 (1989) 1380–1384. doi:10.1021/ic00306a032.

[36]   W.S. Hammack, A.J. Conti, D.N. Hendrickson, H.G. Drickamer, Pressure-Induced Spin-State Interconversion of [Fe(6-Me-py)$_3$tren](ClO$_4$)$_2$ in Solution, J. Am. Chem. Soc. 111 (1989) 1738–1741. doi:10.1021/ja00187a027.

[37]   H. Köppen, E. Meissner, L. Wiehl, H. Spiering, P. Gütlich, Quadrupole splitting of Fe(II) spin crossover compounds study of temperature and pressure dependence and the implication for the interaction mechanism, Hyperfine Interact. 52 (1989) 29–45. doi:10.1007/BF02609561.

[38]   P. Adler, A. Hauser, A. Vef, H. Spiering, P. Gütlich, Dynamics of spin state conversion processes in the solid

state, Hyperfine Interact. 47–48 (1989) 343–356. doi:10.1007/BF02351617.

[39]   P. Adler, H. Spiering, P. Gütlich, Thermodynamics and kinetics of spin state conversion processes studied by pressure dependent mössbauer spectroscopy, J. Phys. Chem. Solids. 50 (1989) 587–597. doi:10.1016/0022-3697(89)90452-6.

[40]   J.K. Beattie, Dynamics of Spin Equilibria in Metal Complexes, Adv. Inorg. Chem. 32 (1988) 1–53. doi:10.1016/S0898-8838(08)60230-5.

[41]   P. Adler, H. Spiering, P. Gütlich, Mössbauer effect study of the temperature and pressure dependence of the singlet-quintet intersystem crossing dynamics in an iron(II) spin crossover complex, Hyperfine Interact. 42 (1988) 1033–1038. doi:10.1007/BF02395567.

[42]   V. Niel, M.C. Muñoz, A.B. Gaspar, A. Galet, G. Levchenko, J.A. Real, Thermal-, pressure-, and light-induced spin transition in novel cyanide-bridged Fe^{II}-Ag^{I} bimetallic compounds with three-dimensional interpenetrating double structures $[Fe^{II}L_x[Ag(CN)_2]_2]·G$, Chem. - A Eur. J. 8 (2002) 2446–2453. doi:10.1002/1521-3765(20020603)8:11<2446::AID-CHEM2446>3.0.CO;2-K.

[43]   M.-L. Boillot, J. Zarembowitch, J.-P. Itie, A. Polian, E. Bourdet, J.G. Haasnoot, Pressure-induced spin-state crossovers at room temperature in iron(II) complexes: comparative analysis; a XANES investigation of some new transitions, New J. Chem. 26 (2002) 313–322. doi:10.1039/b104782p.

[44]   J. Jeftic, A. Hauser, F. Varret, C. Écolivet, Pressure, temperature and light influence on spin transition solids, High Press. Res. 18 (2000) 195–201. doi:10.1080/08957950008200968.

[45]   Y. Garcia, V. Ksenofontov, G. Levchenko, P. Gütlich, Pressure effect on a novel spin transition polymeric chain compound, J. Mater. Chem. 10 (2000) 2274–2276. doi:10.1039/b003794j.

[46]   E. Breuning, M. Ruben, J.-M. Lehn, F. Renz, Y. Garcia, V. Ksenofontov, P. Gütlich, E. Wegelius, K. Rissanen, Spin Crossover in a Supramolecular Fe_4^{II} [2×2] Grid Triggered by Temperature, Pressure, and Light, Angew. Chemie Int. Ed. 39 (2000) 2504–2507. doi:10.1002/1521-3773(20000717)39:14<2504::AID-ANIE2504>3.0.CO;2-B.

[47]   Y. Garcia, V. Ksenofontov, G. Levchenko, G. Schmitt, P. Gütlich, Pressure-Induced High Spin State in $[Fe(btr)_2(NCS)_2]·H_2O$ (btr = 4,4‘-bis-1,2,4-triazole), J. Phys. Chem. B. 104 (2000) 5045–5048. doi:10.1021/jp0004922.

[48]   S. Klokishner, J. Linares, F. Varret, Effect of hydrostatic pressure on phase transitions in spin-crossover 1D systems, Chem. Phys. 255 (2000) 317–323. doi:10.1016/S0301-0104(00)00081-1.

[49]   J. Jeftić, N. Menendez, A. Wack, E. Codjovi, J. Linarès, A. Goujon, G. Hamel, S. Klotz, G. Syfosse, F. Varret, A helium-gas-pressure apparatus with optical- reflectivity detection tested with a spin-transition solid optical detection of the spin transition by reflectivity: application to, Meas. Sci. Technol. 10 (1999). doi:10.1088/0957-0233/10/11/314.

[50]   V. Ksenofontov, H. Spiering, A. Schreiner, G. Levchenko, H.A. Goodwin, P. Gütlich, Influence of hydrostatic

pressure on hysteresis phase transition in spin crossover compounds, J. Phys. Chem. Solids. 60 (1999) 393–399. doi:10.1016/S0022-3697(98)00259-5.

[51] E.C. Constable, G. Baum, E. Bill, R. Dyson, V. Eldik, D. Fenske, S. Kaderli, D. Morris, A. Neubrand, M. Neuburger, D.R. Smith, K. Wieghardt, M. Zehnder, A.D. Zuberbühler, R. van Eldik, Control of Iron(II) Spin States in 2,2′:6′,2″-Terpyridine Complexes through Ligand Substitution, Chem. A Eur. J. 5 (1999) 498–508. doi:10.1002/(sici)1521-3765(19990201)5:2<498::aid-chem498>3.0.co;2-v.

[52] S. Schenker, A. Hauser, W. Wang, I.Y. Chan, High-spin→low-spin relaxation in $[Zn_{1-x}Fe_x(6-mepy)_{3-y}(py)_y tren](PF_6)_2$, J. Chem. Phys. 109 (1998) 9870–9878. doi:10.1063/1.477681.

[53] V. Ksenofontov, G. Levchenko, H. Spiering, P. Gütlich, J.F. Létard, Y. Bouhedja, O. Kahn, Spin crossover behavior under pressure of $Fe(PM-L)_2(NCS)_2$ compounds with substituted 2′-pyridylmethylene 4-anilino ligands, Chem. Phys. Lett. 294 (1998) 545–553. doi:10.1016/S0009-2614(98)00901-4.

[54] G.G. Levchenko, V. Ksenofontov, A. V Stupakov, H. Spiering, Y. Garcia, P. Gütlich, Pressure effect on temperature induced high-spin – low-spin phase transitions, Chem. Phys. 277 (2002) 125–129. doi:10.1016/S0301-0104(01)00707-8.

[55] S. Schenker, A. Hauser, W. Wang, I.. Chan, Matrix effects on the high-spin→low-spin relaxation in $[M_{1-x}Fe_x(bpy)_3](PF_6)_2$ (M=Cd, Mn and Zn, bpy=2,2′-bipyridine), Chem. Phys. Lett. 297 (1998) 281–286. doi:10.1016/S0009-2614(98)01136-1.

[56] Y. Garcia, P.J. van Koningsbruggen, R. Lapouyade, L. Fournès, L. Rabardel, O. Kahn, V. Ksenofontov, G. Levchenko, P. Gütlich, Influences of Temperature, Pressure, and Lattice Solvents on the Spin Transition Regime of the Polymeric Compound $[Fe(hyetrz)_3]A_2·3H_2O$ (hyetrz = 4-(2'-hydroxyethyl)-1,2,4-triazole and A- = 3-nitrophenylsulfonate), Chem. Mater. 10 (1998) 2426–2433. doi:10.1021/CM980107+.

[57] W. Wang, I.Y. Chan, S. Schenker, A. Hauser, Pressure effects on the HS → LS relaxation in $[Zn_{1-x}Fe_x(6-mepy)_3 tren](PF_6)_2$, J. Chem. Phys. 106 (1997) 3817–3820. doi:10.1063/1.473436.

[58] J. Jeftić, A. Hauser, Pressure Study of the Thermal Spin Transition and the High-Spin → Low-Spin Relaxation in the R 3̄ and P 1̄ Crystallographic Phases of $[Zn_{1-x}Fe_x(ptz)_6](BF_4)_2$ Single Crystals (x = 0.1, 0.32, and 1; pt, J. Phys. Chem. B. 101 (1997) 10262–10270. doi:10.1021/jp972083k.

[59] J. Jeftic, R. Hinek, S.C. Capelli, A. Hauser, Cooperativity in the Iron(II) Spin-Crossover Compound $[Fe(ptz)_6](PF_6)_2$ under the Influence of External Pressure (ptz = 1-n-Propyltetrazole)., Inorg. Chem. 36 (1997) 3080–3087. doi:10.1021/ic961404o.

[60] J. Jeftić, U. Kindler, H. Spiering, A. Hauser, Helium gas pressure cell for pressures up to 1 kbar (0.1 GPa) in conjunction with the cold head of a closed-cycle He refrigerator, Meas. Sci. Technol. 8 (1997) 479–483. doi:10.1088/0957-0233/8/5/003.

[61] C. Hannay, M.-J. Hubin-Franskin, F. Grandjean, V. Briois, A. Polian, S. Trofimenko, G.J. Long, X-ray Absorption Spectroscopic Study of the Temperature and Pressure Dependence of the Electronic Spin States in Several Iron(II) and Cobalt(II) Tris(pyrazolyl)borate Complexes, Inorg. Chem. 36 (1997) 5580–5588.

doi:10.1021/ic970506r.

[62] J. Jeftić, H. Romstedt, A. Hauser, The interplay between the spin transition and the crystallographic phase transition in the Fe(II) spin-crossover system [Zn$_{1-x}$Fe$_x$(ptz)$_6$](BF$_4$)$_2$ (x = 0.1, 1; ptz = 1-propyltetrazole), J. Phys. Chem. Solids. 57 (1996) 1743–1750. doi:10.1016/0022-3697(96)00033-9.

[63] J. Jeftić, A. Hauser, The HS → LS relaxation under external pressure in the Fe(II) spin-crossover system [Zn$_{1-x}$Fe$_x$(ptz)$_6$](BF$_4$)$_2$ (ptz = 1-propyltetrazole, x = 0.1), Chem. Phys. Lett. 248 (1996) 458–463. doi:10.1016/0009-2614(95)01297-4.

[64] C. Roux, D.M. Adams, J.P. Itie, A. Polian, D.N. Hendrickson, M. Verdaguer, Pressure-Induced Valence Tautomerism in Cobalt o-Quinone Complexes: An X-ray Absorption Study of the Low-Spin [CoIII(3,5-DTBSQ)(3,5-DTBCat)(phen)] to High-Spin [CoII(3,5-DTBSQ)2(phen)] Interconversion., Inorg. Chem. 35 (1996) 2846–2852. doi:10.1021/IC951080O.

[65] S. Hayami, Y. Hosokoshi, K. Inoue, Y. Einaga, O. Sato, Y. Maeda, Pressure-stabilized low-spin state for binuclear iron(III) spin-crossover compounds, Bull. Chem. Soc. Jpn. 74 (2001) 2361–2368.

[66] C. Roux, J. Zarembowitch, J.-P. Itie, A. Polian, M. Verdaguer, Pressure-Induced Spin-State Crossovers in Six-Coordinate Fe^{II}L$_n$L'$_m$(NCS)$_2$ Complexes with L = L' and L ≠ L': A XANES Investigation., Inorg. Chem. 35 (1996) 574–580. doi:10.1021/IC9507023.

[67] E. König, G. Ritter, H. Grünsteudel, J. Dengler, J. Nelson, Effect of a Simultaneous Change of Temperature and Pressure on the Spin-State Transition in Bis(thiocyanato)bis(2,2'-bi-2-thiazoline)iron(II), Inorg. Chem. 33 (1994) 837–839. doi:10.1021/ic00082a037.

[68] T. Granier, B. Gallois, J. Gaultier, J.A. Real, J. Zarembowitch, High-pressure single-crystal x-ray diffraction study of two spin-crossover iron(II) complexes: Fe(Phen)$_2$(NCS)$_2$ and Fe(Btz)$_2$(NCS)$_2$, Inorg. Chem. 32 (1993) 5305–5312. doi:10.1021/ic00075a058.

[69] J. Zarembowitch, C. Roux, M.L. Boillot, R. Claude, J.P. Itie, A. Polian, M. Bolte, Temperature-, pressure- and light-induced electronic spin conversions in transition metal complexes., Mol. Cryst. Liq. Cryst. Sci. Technol. Sect. A. Mol. Cryst. Liq. Cryst. 234 (1993) 247–254. doi:10.1080/10587259308042923.

[70] C. Roux, J. Zarembowitch, J.P. Itie, M. Verdaguer, E. Dartyge, A. Fontaine, H. Tolentino, Pressure-induced spin-state crossovers in six-coordinate cobalt(II) complexes: a near-edge x-ray absorption study, Inorg. Chem. 30 (1991) 3174–3179. doi:10.1021/ic00016a014.

[71] M. Konno, M. Mikami-Kido, Temperature- or Pressure-Induced Structure Changes of a Spin Crossover Fe(II) Complex; [Fe(bpy)$_2$(NCS)$_2$], Bull. Chem. Soc. Jpn. 64 (1991) 339–345. doi:10.1246/bcsj.64.339.

[72] Y. Sunatsuki, M. Sakata, S. Matsuzaki, N. Matsumoto, M. Kojima, Thermal and Pressure Induced Spin Crossover of a Novel Iron(III) Complex with a Tripodal Ligand Involving Three Imidazole Groups., Chem. Lett. 30 (2001) 1254–1255. doi:10.1246/cl.2001.1254.

[73] V. Ksenofontov, A.B. Gaspar, J.A. Real, P. Gütlich, Pressure-induced spin state conversion in

antiferromagnetically coupled Fe(II) dinuclear complexes, J. Phys. Chem. B. 105 (2001) 12266–12271. doi:10.1021/jp0116961.

[74]   J.K. Grey, I.S. Butler, Effects of high external pressures on the electronic spectra of coordination compounds, Coord. Chem. Rev. 219–221 (2001) 713–759. doi:10.1016/S0010-8545(01)00364-2.

[75]   Y. Garcia, V. Ksenofontov, P. Gütlich, New polynuclear 4,4′-bis-1,2,4-triazole Fe(II) spin crossover compounds, Comptes Rendus l'Academie Des Sci. - Ser. IIc Chem. 4 (2001) 227–233. doi:10.1016/S1387-1609(00)01222-6.

[76]   P. Guionneau, C. Brigouleix, Y. Barrans, A.E. Goeta, J.-F. Létard, J.A.. Howard, J. Gaultier, D. Chasseau, High pressure and very low temperature effects on the crystal structures of some iron(II) complexes, Comptes Rendus l'Académie Des Sci. - Ser. IIC - Chem. 4 (2001) 161–171. doi:10.1016/S1387-1609(00)01193-2.

[77]   E. Codjovi, N. Menéndez, J. Jeftic, F. Varret, Pressure and temperature hysteresis in the spin- transition solid $Fe(btr)_2(NCS)_2 \cdot H_2O$, pure and diluted in Ni matrix, Comptes Rendus l'Academie Des Sci. - Ser. IIc Chem. 4 (2001) 181–188. doi:10.1016/S1387-1609(00)01221-4.

[78]   P. Guionneau, M. Marchivie, Y. Garcia, J.A.K. Howard, D. Chasseau, Spin crossover in $[Mn^{III}(pyrol)_3tren]$ probed by high-pressure and low-temperature x-ray diffraction, Phys. Rev. B. 72 (2005) 214408. doi:10.1103/PhysRevB.72.214408.

[79]   H.J. Shepherd, S. Bonnet, P. Guionneau, S. Bedoui, G. Garbarino, W. Nicolazzi, A. Bousseksou, G. Molnár, Pressure-induced two-step spin transition with structural symmetry breaking: X-ray diffraction, magnetic, and Raman studies, Phys. Rev. B - Condens. Matter Mater. Phys. 84 (2011). doi:10.1103/PhysRevB.84.144107.

[80]   H.J. Shepherd, High pressure structural detail provides insight into molecular spin state switching, Diam. Light Source Annu. Rev. (2013) 109.

[81]   J. Jeftić, C. Ecolivet, A. Hauser, External Pressure and Light Influence on Internal Pressure in a Spin-Crossover Solid $[Zn:Fe(ptz)_6](BF_4)_2$, High Press. Res. 23 (2003) 359–363. doi:10.1080/0895795031000139127.

[82]   P. Gütlich, V. Ksenofontov, A.B. Gaspar, Pressure effect studies on spin crossover systems, Coord. Chem. Rev. 249 (2005) 1811–1829. doi:10.1016/j.ccr.2005.01.022.

[83]   W. a. Bassett, Diamond anvil cell, 50th birthday, High Press. Res. 29 (2009) 163–186. doi:10.1080/08957950802597239.

[84]   J. Badro, G. Fiquet, F. Guyot, J.P. Rueff, V. V. Struzhkin, G. Vankó, G. Monaco, Iron partitioning in earth's mantle: Toward a deep lower mantle discontinuity, Science (80-.). 300 (2003) 789–791. doi:10.1126/science.1081311.

[85]   V. Cerantola, C. McCammon, I. Kupenko, I. Kantor, C. Marini, M. Wilke, L. Ismailova, N. Solopova, A. Chumakov, S. Pascarelli, L. Dubrovinsky, High-pressure spectroscopic study of siderite ($FeCO_3$) with a focus on spin crossover, Am. Mineral. 100 (2015) 2670–2681. doi:10.2138/am-2015-5319.

[86]   R.J. Angel, M. Bujak, J. Zhao, G.D. Gatta, S.D. Jacobsen, Effective hydrostatic limits of pressure media for

high-pressure crystallographic studies, J. Appl. Cryst. J. Appl. Cryst. 40 (2007) 26–32. doi:10.1107/S0021889806045523.

[87]   S. Klotz, J.C. Chervin, P. Munsch, G. Le Marchand, Hydrostatic limits of 11 pressure transmitting media, J. Phys. D. Appl. Phys. 42 (2009) 075413. doi:10.1088/0022-3727/42/7/075413.

[88]   G. Molnár, T. Kitazawa, L. Dubrovinsky, J.J. McGarvey, A. Bousseksou, Pressure tuning Raman spectroscopy of the spin crossover coordination polymer Fe(C5H5N)2Ni(CN)4, J. Physics-Condensed Matter. 16 (2004) S1129–S1136. doi:10.1088/0953-8984/16/14/022.

[89]   G.J. Piermarini, S. Block, J.D. Barnett, R.A. Forman, Calibration of the pressure dependence of the R_1 ruby fluorescence line to 195 kbar, J. Appl. Ph. 46 (1975) 2774–2780. doi:10.1063/1.321957.

[90]   K. Syassen, High Pressure Research An International Journal Ruby under pressure, High Press. Res. 28 (2008) 75–126. doi:10.1080/08957950802235640.

[91]   R.J. Angel, D.R. Allan, R. Miletich, L.W. Finger, The Use of Quartz as an Internal Pressure Standard in High-Pressure Crystallography, J. Appl. Crystallogr. 30 (1997) 461–466. doi:10.1107/S0021889897000861.

[92]   A. Eiling, J.S. Schilling, Pressure and temperature dependence of electrical resistivity of Pb and Sn from 1-300K and 0-10 GPa-use as continuous resistive pressure monitor accurate over wide temperature range; Superconductivity under pressure in Pb, Sn and in, J. Phys. F Met. Phys. 11 (1981) 623–639. doi:10.1088/0305-4608/11/3/010.

[93]   M.I. Eremets, High Pressure Experimental Methods, Oxford University, 1997.

[94]   L. Merrill, W.A. Bassett, Miniature diamond anvil pressure cell for single crystal x-ray diffraction studies, Rev. Sci. Instrum. 45 (1974) 290–294. doi:10.1063/1.1686607.

[95]   R. Letoullec, J.P. Pinceaux, P. Loubeyre, The membrane diamond anvil cell: A new device for generating continuous pressure and temperature variations, High Press. Res. 1 (1988) 77–90. doi:10.1080/08957958808202482.

[96]   S.A. Moggach, D.R. Allan, S. Parsons, J.E. Warren, Incorporation of a new design of backing seat and anvil in a Merrill-Bassett diamond anvil cell, J. Appl. Crystallogr. 41 (2008) 249–251. doi:10.1107/S0021889808000514.

[97]   J. Gaultier, T. Granier, B. Gallois, J.A. Real, J. Zarembowitch, High pressure single crystal X-ray diffraction study of the spin crossover iron(II) complex Fe(Phen)2(NCS)2, High Press. Res. 7 (1991) 336–338. doi:10.1080/08957959108245585.

[98]   P. Guionneau, D. Le Pévelen, M. Marchivie, S. Pechev, J. Gaultier, Y. Barrans, D. Chasseau, Laboratory high-pressure single-crystal x-ray diffraction—recent improvements and examples of studies, J. Phys. Condens. Matter. 16 (2004) S1151–S1159. doi:10.1088/0953-8984/16/14/025.

[99]   A.D. Rosa, M. Merkulova, G. Garbarino, V. Svitlyk, J. Jacobs, C.J. Sahle, O. Mathon, M. Munoz, S. Merkel, High Pressure Research, High Press. Res. 36 (2017) 564–574. doi:10.1080/08957959.2016.1245297.

[100] D.J. Dunstan, Theory of the gasket in diamond anvil high-pressure cells, Rev. Sci. Instrum. 60 (1989) 3789–3795. doi:10.1063/1.1140442.

[101] H.E. Lorenzana, M. Bennahmias, H. Radousky, M.B. Kruger, Producing diamond anvil cell gaskets for ultrahigh-pressure applications using an inexpensive electric discharge machine, Rev. Sci. Instrum. 65 (1994) 3540–3543. doi:10.1063/1.1144535.

[102] M. Mito, M. Hitaka, T. Kawae, K. Takeda, T. Kitai, N. Toyoshima, Development of Miniature Diamond Anvil Cell for the Superconducting Quantum Interference Device Magnetometer, Jpn. J. Appl. Phys. 40 (2001) 6641–6644. doi:10.1143/JJAP.40.6641.

[103] G. Giriat, W. Wang, J.P. Attfield, A.D. Huxley, K. V. Kamenev, Turnbuckle diamond anvil cell for high-pressure measurements in a superconducting quantum interference device magnetometer, Rev. Sci. Instrum. 81 (2010) 073905. doi:10.1063/1.3465311.

[104] D. Pinkowicz, M. Rams, M. Mišek, K. V. Kamenev, H. Tomkowiak, A. Katrusiak, B. Sieklucka, Enforcing Multifunctionality: A Pressure-Induced Spin-Crossover Photomagnet, J. Am. Chem. Soc. 137 (2015) 8795–8802. doi:10.1021/jacs.5b04303.

[105] J.M. Besson, G. Hamel, T. Grima, R.J. Nelmes, J.S. Loveday, S. Hull, D. Häusermann, A large volume pressure cell for high temperatures, High Press. Res. 8 (1992) 625–630. doi:10.1080/08957959208206312.

[106] S. Zhai, E. Ito, Recent advances of high-pressure generation in a multianvil apparatus using sintered diamond anvils, Geosci. Front. 2 (2011) 101–106. doi:10.1016/J.GSF.2010.09.005.

[107] H. Fujiwara, H. Kadomatsu, K. Tohma, Simple clamp pressure cell up to 30 kbar, Rev. Sci. Instrum. 51 (1980) 1345–1348. doi:10.1063/1.1136061.

[108] I.R. Walker, Nonmagnetic piston–cylinder pressure cell for use at 35 kbar and above, Rev. Sci. Instrum. 70 (1999) 3402–3412. doi:10.1063/1.1149927.

[109] X. Wang, K. V. Kamenev, Review of modern instrumentation for magnetic measurements at high pressure and low temperature, Low Temp. Phys. 40 (2014) 735–746. doi:10.1063/1.4892645.

[110] A. Bousseksou, G. Molnár, J.P. Tuchagues, N. Menéndez, É. Codjovi, F. Varret, Triggering the spin-crossover of Fe(phen)$_2$(NCS)$_2$ by a pressure pulse. Pressure and magnetic field induce "mirror effects," Comptes Rendus Chim. 6 (2003) 329–335. doi:10.1016/S1631-0748(03)00042-0.

[111] G. Molnár, V. Niel, J.A. Real, L. Dubrovinsky, A. Bousseksou, J.J. Mcgarvey, Raman Spectroscopic Study of Pressure Effects on the Spin-Crossover Coordination Polymers Fe(Pyrazine)[M(CN)$_4$.2H$_2$O (M = Ni, Pd, Pt). First Observation of a Piezo-Hysteresis Loop at Room Temperature, J. Phys. Chem. B. 107 (2003) 3149–3155. doi:10.1021/jp027550z.

[112] A. Diaconu, S.L. Lupu, I. Rusu, I.M. Risca, L. Salmon, G. Molnár, A. Bousseksou, P. Demont, A. Rotaru, Piezoresistive Effect in the [Fe(Htrz)$_2$(trz)](BF$_4$) Spin Crossover Complex, J. Phys. Chem. Lett. 8 (2017) 3147–3151. doi:10.1021/acs.jpclett.7b01111.

[113] D.S. Yufit, J.A.K. Howard, Simple pressure cell for single-crystal X-ray crystallography, J. Appl. Cryst. 38 (2005) 583–586. doi:10.1107/S0021889805011258.

[114] N. Paradis, F. Le Gac, P. Guionneau, A. Largeteau, D. Yufit, P. Rosa, J.-F. Létard, G. Chastanet, Effects of Internal and External Pressure on the [Fe(PM-PEA)$_2$(NCS)$_2$] Spin-Crossover Compound (with PM-PEA = N-(2′-pyridylmethylene)-4-(phenylethynyl)aniline), Magnetochemistry. 2 (2016) 15. doi:10.3390/magnetochemistry2010015.

[115] G.A. Craig, J.S. Costa, O. Roubeau, S.J. Teat, H.J. Shepherd, M. Lopes, G. Molnár, A. Bousseksou, G. Aromi, High-temperature photo-induced switching and pressure-induced transition in a cooperative molecular spin-crossover material, Dalt. Trans. 43 (2014) 729–737. doi:10.1039/C3DT52075G.

[116] P. Guionneau, E. Collet, Piezo- and Photo-Crystallography Applied to Spin-Crossover Materials, in: Spin-Crossover Mater., John Wiley & Sons Ltd, Oxford, UK, 2013: pp. 507–526. doi:10.1002/9781118519301.ch20.

[117] A. Dawson, D.R. Allan, S. Parsons, M. Ruf, Use of a CCD diffractometer in crystal structure determinations at high pressure, J. Appl. Crystallogr. 37 (2004) 410–416. doi:10.1107/S0021889804007149.

[118] A. Katrusiak, P.F. McMillan, North Atlantic Treaty Organization. Scientific Affairs Division., High-pressure crystallography, Kluwer Academic Publishers, 2004.

[119] C.P. Brock, J.D. Dunitz, Towards a Grammar of Crystal Packing, Chem. Mater. 6 (1994) 1118–1127. doi:10.1021/cm00044a010.

[120] H. Ahsbahs, High pressure cell for use on four-circle diffractometers, Rev. Phys. Appliquée. 19 (1984) 819–821. doi:10.1051/rphysap:01984001909081900.

[121] N. Casati, P. Macchi, A. Sironi, Molecular crystals under high pressure: theoretical and experimental investigations of the solid-solid phase transitions in [Co$_2$(CO)$_6$(XPh$_3$)$_2$] (X = P, As)., Chemistry. 15 (2009) 4446–57. doi:10.1002/chem.200801528.

[122] H. Jin, C.H. Woodall, X. Wang, S. Parsons, K. V Kamenev, A novel diamond anvil cell for x-ray diffraction at cryogenic temperatures manufactured by 3D printing, Cit. Rev. Sci. Instruments. 88 (2017) 35103. doi:10.1063/1.4977486.

[123] V. Legrand, F. Le Gac, P. Guionneau, J.-F. Létard, Neutron powder diffraction studies of two spin transition Fe^{II} complexes under pressure, J. Appl. Crystallogr. 41 (2008) 637–640. doi:10.1107/S0021889808006481.

[124] V. Legrand, S. Pechev, J.-F. Létard, P. Guionneau, Synergy between polymorphism, pressure, spin-crossover and temperature in [Fe(PM-BiA)$_2$(NCS)$_2$]: a neutron powder diffraction investigation, Phys. Chem. Chem. Phys. Phys. Chem. Chem. Phys. 15 (2013) 13872–13880. doi:10.1039/c3cp51444g.

[125] J.A. Wolny, R. Diller, V. Schünemann, Vibrational spectroscopy of mono- and polynuclear spin-crossover systems, Eur. J. Inorg. Chem. (2012) 2635–2648. doi:10.1002/ejic.201200059.

[126] H.J. Shepherd, G. Tonge, L. Hatcher, M. Bryant, J. Knichal, P. Raithby, M. Halcrow, R. Kulmaczewski, K. Gagnon, S. Teat, A High Pressure Investigation of the Order-Disorder Phase Transition and Accompanying Spin

Crossover in [FeL$_{12}$](ClO$_4$)$_2$ (L1 = 2,6-bis{3-methylpyrazol-1-yl}-pyrazine), Magnetochemistry. 2 (2016) 9. doi:10.3390/magnetochemistry2010009.

[127]   H.J. Shepherd, T. Palamarciuc, P. Rosa, P. Guionneau, G. Molnár, J.F. Létard, A. Bousseksou, Antagonism between extreme negative linear compression and spin crossover in [Fe(dpp)$_2$(NCS)$_2$]·py, Angew. Chemie - Int. Ed. 51 (2012) 3910–3914. doi:10.1002/anie.201108919.

[128]   D.M. Adams, S.J. Payne, K. Martin, The Fluorescence of Diamond and Raman Spectroscopy at High Pressures Using a New Design of Diamond Anvil Cell, Appl. Spectrosc. 27 (1973) 377–381. doi:10.1366/000370273774333353.

[129]   J.C. Chervin, B. Canny, J.M. Besson, P. Pruzan, A diamond anvil cell for IR microspectroscopy, Rev. Sci. Instrum. 66 (1995) 2595–2598. doi:10.1063/1.1145594.

[130]   V. Ksenofontov, G. Levchenko, S. Reiman, P. Gütlich, A. Bleuzen, V. Escax, M. Verdaguer, Pressure-induced electron transfer in ferrimagnetic Prussian blue analogs, Phys. Rev. B. 68 (2003) 024415. doi:10.1103/PhysRevB.68.024415.

[131]   A.X. Trautwein, H. Paulsen, H. Winkler, H. Giefers, G. Wortmann, H. Toftlund, J.A. Wolny, A.I. Chumakov, O. Leupold, Pressure-induced changes of the vibrational modes of spin-crossover complexes studied by nuclear resonance scattering of synchrotron radiation, in: J. Phys. Conf. Ser., 2010. doi:10.1088/1742-6596/217/1/012125.

[132]   G. Levchenko, G. V. Bukin, S.A. Terekhov, A.B. Gaspar, V. Martínez, M.C. Muñoz, J.A. Real, Pressure-Induced Cooperative Spin Transition in Iron(II) 2D Coordination Polymers: Room-Temperature Visible Spectroscopic Study, J. Phys. Chem. B. 115 (2011) 8176–8182. doi:10.1021/jp201585x.

[133]   A. Galet, A.B. Gaspar, M.C. Muñoz, G. V. Bukin, G. Levchenko, J.A. Real, Tunable bistability in a three-dimensional spin-crossover sensory- and memory-functional material, Adv. Mater. 17 (2005) 2949–2953. doi:10.1002/adma.200501122.

[134]   A. Galet, A.B. Gaspar, G. Agusti, M.C. Muñoz, G. Levchenko, J.A. Real, Pressure Effect Investigations on the Spin Crossover Systems{Fe[H$_2$B(pz)$_2$]$_2$(bipy)} and {Fe[H$_2$B(pz)$_2$]$_2$(phen)}, Eur. J. Inorg. Chem. 2006 (2006) 3571–3573. doi:10.1002/ejic.200600517.

[135]   V. Martínez, A.B. Gaspar, M. Carmen Muñoz, G. V. Bukin, G. Levchenko, J.A. Real, Synthesis and characterisation of a new series of bistable iron(II) spincrossover 2D metal-organic frameworks, Chem. - A Eur. J. 15 (2009) 10960–10971. doi:10.1002/chem.200901391.

[136]   H. Spiering, K. Boukheddaden, J. Linares, F. Varret, Total free energy of a spin-crossover molecular system, Phys. Rev. B - Condens. Matter Mater. Phys. 70 (2004) 1–15. doi:10.1103/PhysRevB.70.184106.

[137]   V. Ksenofontov, A.B. Gaspar, G. Levchenko, B. Fitzsimmons, P. Gütlich, Pressure Effect on Spin Crossover in [Fe(phen)$_2$(NCS)$_2$] and [CrI$_2$(depe)$_2$], J. Phys. Chem. B. 108 (2004) 7723–7727. doi:10.1021/jp049512g.

[138]   A.B. Gaspar, G. Agustí, V. Martínez, M.C. Muñoz, G. Levchenko, J.A. Real, Spin crossover behaviour in the

iron(II)-2,2-dipyridilamine system: Synthesis, X-ray structure and magnetic studies, Inorganica Chim. Acta. 358 (2005) 4089–4094. doi:10.1016/J.ICA.2005.06.022.

[139] A.B. Gaspar, M.C. Muñoz, N. Moliner, V. Ksenofontov, G. Levchenko, P. Gütlich, J.A. Real, Polymorphism and Pressure Driven Thermal Spin Crossover Phenomenon in $[Fe(abpt)_2(NCX)_2]$ (X = S, and Se): Synthesis, Structure and Magnetic Properties, Monatshefte Fur Chemie. 134 (2003) 285–294. doi:10.1007/s00706-002-0508-5.

[140] B. Li, R.-J. Wei, J. Tao, R.-B. Huang, L.-S. Zheng, Pressure Effects on a Spin-Crossover Monomeric Compound $[Fe(pmea)(SCN)_2]$ (pmea = bis[(2-pyridyl)methyl]-2-(2-pyridyl)ethylamine), Inorg. Chem. 49 (2010) 745–751. doi:10.1021/ic902161v.

[141] A. Sugahara, K. Moriya, M. Enomoto, A. Okazawa, N. Kojima, Study on the spin-crossover transition in [Fe(cis-/trans-stpy)$_4$(X)$_2$] (stpy: styrylpyridine, X: NCS, NCBH$_3$) under high pressure toward ligand-driven light-induced spin change, Polyhedron. 30 (2011) 3127–3130. doi:10.1016/J.POLY.2011.03.008.

[142] F.-L. Yang, B. Li, T. Hanajima, Y. Einaga, R.-B. Huang, L.-S. Zheng, J. Tao, An iron(II) incomplete spin-crossover compound: pressure effects and Mössbauer spectroscopy study., Dalton Trans. 39 (2010) 2288–2292. doi:10.1039/b917518k.

[143] N.F. Sciortino, S.M. Neville, C. Desplanches, J.-F. Létard, V. Martinez, J.A. Real, B. Moubaraki, K.S. Murray, C.J. Kepert, An Investigation of Photo- and Pressure-Induced Effects in a Pair of Isostructural Two-Dimensional Spin-Crossover Framework Materials, Chem. - A Eur. J. 20 (2014) 7448–7457. doi:10.1002/chem.201400367.

[144] H. Romstedt, A. Hauser, H. Spiering, High-spin → low-spin relaxation in the two-step spincrossover compound $[Fe(pic)_3]Cl_2EtOH$ (pic = 2-picolylamine), J. Phys. Chem. Solids. 59 (1998) 265–275. doi:10.1016/S0022-3697(97)00142-X.

[145] A. Rotaru, F. Varret, E. Codjovi, K. Boukheddaden, J. Linares, A. Stancu, P. Guionneau, J.-F. Létard, Hydrostatic pressure investigation of the spin crossover compound $[Fe(PM{-}BiA)_2(NCS)_2]$ polymorph I using reflectance detection, J. Appl. Phys. 106 (2009) 053515. doi:10.1063/1.3202385.

[146] V. Martínez, Z.A. Castillo, M.C. Muñoz, A.B. Gaspar, C. Etrillard, J.F. Létard, S.A. Terekhov, G. V. Bukin, G. Levchenko, J.A. Real, Thermal-, pressure-and light-induced spin-crossover behaviour in the two-dimensional hofmann-like coordination polymer $[Fe(3-Clpy)_2Pd(CN)_4]$, Eur. J. Inorg. Chem. 2013 (2013) 813–818. doi:10.1002/ejic.201201097.

[147] A.B. Gaspar, G. Levchenko, S. Terekhov, G. Bukin, J. Valverde-Muñoz, F.J. Muñoz-Lara, M. Seredyuk, J.A. Real, The effect of pressure on the cooperative spin transition in the 2D coordination polymer $\{Fe(phpy)_2[Ni(CN)_4]\}$, Eur. J. Inorg. Chem. 2014 (2014) 429–433. doi:10.1002/ejic.201301374.

[148] G. Levchenko, A. Khristov, V. Kuznetsova, V. Shelest, Pressure and temperature induced high spin–low spin phase transition: Macroscopic and microscopic consideration, J. Phys. Chem. Solids. 75 (2014) 966–971. doi:10.1016/J.JPCS.2014.04.006.

[149] A.B. Gaspar, M.C. Muñoz, J.A. Real, Dinuclear iron^{II} spin crossover compounds: singular molecular materials

for electronics, J. Mater. Chem. 16 (2006) 2522–2533. doi:10.1039/B603488H.

[150] J.J.M. Amoore, C.J. Kepert, J.D. Cashion, B. Moubaraki, S.M. Neville, K.S. Murray, Structural and Magnetic Resolution of a Two-Step Full Spin-Crossover Transition in a Dinuclear Iron(II) Pyridyl-Bridged Compound, Chem. - A Eur. J. 12 (2006) 8220–8227. doi:10.1002/chem.200601069.

[151] W. Bauer, W. Scherer, S. Altmannshofer, B. Weber, Two-step versus one-step spin transitions in iron(II) 1D chain compounds, Eur. J. Inorg. Chem. (2011) 2803–2818. doi:10.1002/ejic.201001363.

[152] J. Bin Lin, W. Xue, B.Y. Wang, J. Tao, W.X. Zhang, J.P. Zhang, X.M. Chen, Chemical/physical pressure tunable spin-transition temperature and hysteresis in a two-step spin crossover porous coordination framework, Inorg. Chem. 51 (2012) 9423–9430. doi:10.1021/ic301237p.

[153] H.J. Shepherd, C. Bartual-Murgui, G. Molnár, J.A. Real, M.C. Muñoz, L. Salmon, A. Bousseksou, Thermal and pressure-induced spin crossover in a novel three-dimensional Hoffman-like clathrate complex, New J. Chem. 35 (2011) 1205–1210. doi:10.1039/c0nj00845a.

[154] B. Schneider, S. Demeshko, S. Dechert, F. Meyer, A Double-Switching Multistable Fe_4 Grid Complex with Stepwise Spin-Crossover and Redox Transitions, Angew. Chemie Int. Ed. 49 (2010) 9274–9277. doi:10.1002/anie.201001536.

[155] T. Matsumoto, G.N. Newton, T. Shiga, S. Hayami, Y. Matsui, H. Okamoto, R. Kumai, Y. Murakami, H. Oshio, Programmable spin-state switching in a mixed-valence spin-crossover iron grid, Nat. Commun. 5 (2014) 3865. doi:10.1038/ncomms4865.

[156] M.J. Murphy, K.A. Zenere, F. Ragon, P.D. Southon, C.J. Kepert, S.M. Neville, Guest Programmable Multistep Spin Crossover in a Porous 2-D Hofmann-Type Material, (n.d.). doi:10.1021/jacs.6b12465.

[157] M. Griffin, S. Shakespeare, H.J. Shepherd, C.J. Harding, J.-F. Létard, C. Desplanches, A.E. Goeta, J.A.K. Howard, A.K. Powell, V. Mereacre, Y. Garcia, A.D. Naik, H. Müller-Bunz, G.G. Morgan, A symmetry-breaking spin-state transition in iron(III), Angew. Chemie - Int. Ed. 50 (2011). doi:10.1002/anie.201005545.

[158] H. Spiering, Elastic Interaction in Spin-Crossover Compounds, in: Spin Crossover Transit. Met. Compd. III, 2004: pp. 171–195. doi:10.1007/b95427.

[159] S. Zein, S.A. Borshch, Energetics of binuclear spin transition complexes, J. Am. Chem. Soc. 127 (2005) 16197–16201. doi:10.1021/ja054282k.

[160] E.M. Zueva, E.R. Ryabikh, S.A. Borshch, Theoretical Analysis of Spin Crossover in Iron(II) [2 × 2] Molecular Grids, Inorg. Chem. 50 (2011) 11143–11151. doi:10.1021/ic2016929.

[161] M. Paez-Espejo, M. Sy, K. Boukheddaden, Elastic Frustration Causing Two-Step and Multistep Transitions in Spin-Crossover Solids: Emergence of Complex Antiferroelastic Structures, J. Am. Chem. Soc. 138 (2016) 3202–3210. doi:10.1021/jacs.6b00049.

[162] J.A. Real, H. Bolvin, A. Bousseksou, A. Dworkin, O. Kahn, F. Varret, J. Zarembowitch, Two-step spin crossover in the new dinuclear compound [Fe(bt)(NCS)$_2$]$_2$bpym, with bt = 2,2'-bi-2-thiazoline and bpym = 2,2'-

bipyrimidine: experimental investigation and theoretical approach, J. Am. Chem. Soc. 114 (1992) 4650–4658. doi:10.1021/ja00038a031.

[163] D. Chernyshov, M. Hostettler, K.W. Törnroos, H.-B. Bürgi, Ordering Phenomena and Phase Transitions in a Spin-Crossover Compound—Uncovering the Nature of the Intermediate Phase of[Fe(2-pic)$_3$]Cl$_2$·EtOH, Angew. Chemie Int. Ed. 42 (2003) 3825–3830. doi:10.1002/anie.200351834.

[164] V. Ksenofontov, A.B. Gaspar, V. Niel, S. Reiman, J.A. Real, P. Gütlich, On the Nature of the Plateau in Two-Step Dinuclear Spin-Crossover Complexes, Chem. - A Eur. J. 10 (2004) 1291–1298. doi:10.1002/chem.200305275.

[165] A. Bousseksou, F. Varret, J. Nasser, Ising-like model for the two step spin-crossover of binuclear molecules, J. Phys. I. 3 (1993) 1463–1473. doi:10.1051/jp1:1993191.

[166] E. Milin, V. Patinec, S. Triki, E.-E. Bendeif, S. Pillet, M. Marchivie, G. Chastanet, K. Boukheddaden, Elastic Frustration Triggering Photoinduced Hidden Hysteresis and Multistability in a Two-Dimensional Photoswitchable Hofmann-Like Spin-Crossover Metal–Organic Framework, Inorg. Chem. 55 (2016) 11652–11661. doi:10.1021/acs.inorgchem.6b01081.

[167] A. Bhattacharjee, V. Ksenofontov, J.A. Kitchen, N.G. White, S. Brooker, P. Gütlich, Effect of pressure and light on the spin transition behavior of the dinuclear iron(II) compound [Fe$^{II}_2$(PMAT)$_2$](BF$_4$)$_4$.DMF, Appl. Phys. Lett. 92 (2008) 174104. doi:10.1063/1.2911918.

[168] B. Li, R.J. Wei, J. Tao, R. Bin Huang, L.S. Zheng, Z. Zheng, Solvent-induced transformation of single crystals of a spin-crossover (SCO) compound to single crystals with two distinct SCO centers, J. Am. Chem. Soc. 132 (2010) 1558–1566. doi:10.1021/ja909695f.

[169] G. Molnár, T. Guillon, N.O. Moussa, L. Rechignat, T. Kitazawa, M. Nardone, A. Bousseksou, Two-step spin-crossover phenomenon under high pressure in the coordination polymer Fe(3-methylpyridine)$_2$[Ni(CN)$_4$], (2006). doi:10.1016/j.cplett.2006.03.053.

[170] N.F. Sciortino, F. Ragon, K.A. Zenere, P.D. Southon, G.J. Halder, K.W. Chapman, L. Piñeiro-López, J.A. Real, C.J. Kepert, S.M. Neville, Exploiting Pressure to Induce a "guest-Blocked" Spin Transition in a Framework Material, Inorg. Chem. 55 (2016) 10490–10498. doi:10.1021/acs.inorgchem.6b01686.

[171] Y. Garcia, P. Gütlich, Thermal Spin Crossover in Mn(II), Mn(III), Cr(II) and Co(III) Coordination Compounds, Spin Crossover Transit. Met. Compd. II. (2004) 49–62. doi:10.1007/b95412.

[172] D.M. Halepoto, D.G.L. Holt, L.F. Larkworthy, G.J. Leigh, D.C. Povey, G.W. Smith, Spin crossover in chromium(II) complexes and the crystal and molecular structure of the high spin form of bis[1,2-bis(diethylphosphino)ethane]di-iodochromium(II), J. Chem. Soc. Chem. Commun. 0 (1989) 1322. doi:10.1039/c39890001322.

[173] P.Á. Szilágyi, S. Dorbes, G. Molnár, J.A. Real, Z. Homonnay, C. Faulmann, A. Bousseksou, Temperature and pressure effects on the spin state of ferric ions in the [Fe(sal2-trien)][Ni(dmit)$_2$] spin crossover complex, J. Phys. Chem. Solids. 69 (2008) 2681–2686. doi:10.1016/j.jpcs.2008.06.106.

[174] A. Tissot, H.J. Shepherd, L. Toupet, E. Collet, J. Sainton, G. Molnár, P. Guionneau, M.L. Boillot, Temperature- and pressure-induced switching of the molecular spin state of an orthorhombic iron(III) spin-crossover salt, Eur. J. Inorg. Chem. (2013) 1001–1008. doi:10.1002/ejic.201201059.

[175] V.J. Cornelius, P.J. Titler, G.R. Fern, J.R. Miller, J. Silver, M.J. Snowden, C.A. McCammon, An Interesting Spin-State Transition for [Fe(PPIX)OH] Induced by High Pressure in a Diamond Anvil Cell, Hyperfine Interact. 144/145 (2002) 359–363. doi:10.1023/A:1025440108151.

[176] H. Spiering, E. Meissner, H. Köppen, E.W. Müller, P. Gütlich, The effect of the lattice expansion on high spin $\rightleftharpoons$ low spin transitions, Chem. Phys. 68 (1982) 65–71. doi:10.1016/0301-0104(82)85080-5.

[177] S. Bonhommeau, G. Molnár, M. Goiran, K. Boukheddaden, A. Bousseksou, Unified dynamical description of pulsed magnetic field and pressure effects on the spin crossover phenomenon, Phys. Rev. B - Condens. Matter Mater. Phys. 74 (2006) 1–8. doi:10.1103/PhysRevB.74.064424.

[178] C.-M. Jureschi, I. Rusu, E. Codjovi, J. Linares, Y. Garcia, A. Rotaru, Thermo- and piezochromic properties of [Fe(hyptrz)]A$_2$·H$_2$O spin crossover 1D coordination polymer: Towards spin crossover based temperature and pressure sensors, Phys. B Condens. Matter. 449 (2014) 47–51. doi:10.1016/J.PHYSB.2014.04.081.

[179] J.A. Nasser, K. Boukheddaden, J. Linares, Two-step spin conversion and other effects in the atom-phonon coupling model, Eur. Phys. J. B. 39 (2004) 219–227. doi:10.1140/epjb/e2004-00184-y.

[180] K. Boukheddaden, S. Miyashita, M. Nishino, Elastic interaction among transition metals in one-dimensional spin-crossover solids, Phys. Rev. B. 75 (2007) 094112. doi:10.1103/PhysRevB.75.094112.

[181] A. Rotaru, J. Linares, E. Codjovi, J. Nasser, A. Stancu, Size and pressure effects in the atom-phonon coupling model for spin crossover compounds, J. Appl. Phys. 103 (2008) 07B908. doi:10.1063/1.2832674.

[182] Y. Konishi, H. Tokoro, M. Nishino, S. Miyashita, Monte Carlo simulation of pressure-induced phase transitions in spin-crossover materials, Phys. Rev. Lett. 100 (2008) 18–21. doi:10.1103/PhysRevLett.100.067206.

[183] C. Enachescu, L. Stoleriu, A. Stancu, A. Hauser, Model for Elastic Relaxation Phenomena in Finite 2D Hexagonal Molecular Lattices, Phys. Rev. Lett. 102 (2009) 257204. doi:10.1103/PhysRevLett.102.257204.

[184] S. Miyashita, Y. Konishi, M. Nishino, H. Tokoro, P.A. Rikvold, Realization of the mean-field universality class in spin-crossover materials, Phys. Rev. B. 77 (2008) 014105. doi:10.1103/PhysRevB.77.014105.

[185] C.R. Pike, A.P. Roberts, K.L. Verosub, Characterizing interactions in fine magnetic particle systems using first order reversal curves, J. Appl. Phys. 85 (1999) 6660–6667. doi:10.1063/1.370176.

[186] A. Rotaru, J. Linares, F. Varret, E. Codjovi, A. Slimani, R. Tanasa, C. Enachescu, A. Stancu, J. Haasnoot, Pressure effect investigated with first-order reversal-curve method on the spin-transition compounds [Fe$_x$Zn$_{1-x}$(btr)$_2$(NCS)<sub>2<sub>]·H$_2$O (x = 0.6, 1), Phys. Rev. B. 83 (2011) 224107. doi:10.1103/PhysRevB.83.224107.

[187] M. Mikolasek, M.D. Manrique-Juarez, H.J. Shepherd, K. Ridier, S. Rat, V. Shalabaeva, A.-C. Bas, I.E. Collings, F. Mathieu, J. Cacheux, T. Leichlé, L. Nicu, W. Nicolazzi, L. Salmon, G. Molnár, A. Bousseksou, A Complete

Set of Elastic Moduli of a Spin-Crossover Solid: Spin-State Dependence and Mechanical Actuation, J. Am. Chem. Soc. (2018) jacs.8b05347. doi:10.1021/jacs.8b05347.

[188] H.J. Shepherd, I.A. Gural'skiy, C.M. Quintero, S. Tricard, L. Salmon, G. Molnár, A. Bousseksou, Molecular actuators driven by cooperative spin-state switching, Nat. Commun. 4 (2013) 2607. doi:10.1038/ncomms3607.

[189] G. Molnár, S. Rat, L. Salmon, W. Nicolazzi, A. Bousseksou, Spin Crossover Nanomaterials: From Fundamental Concepts to Devices, Adv. Mater. (2017) 17003862. doi:10.1002/adma.201703862.